OPEN ACCESS

University of BRISTOL

Hs, C. J., Champneys, A. R., Paul, K., & McNeely, M. (2017). Dynamic behaviour of direct spring loaded pressure relief valves connected to inlet piping: IV review and recommendations. *Journal of Loss Prevention in the Process Industries*. https://doi.org/10.1016/j.jlp.2017.04.005

Peer reviewed version

License (if available):
Unspecified

Link to published version (if available):
10.1016/j.jlp.2017.04.005

Link to publication record in Explore Bristol Research
PDF-document

This is the author accepted manuscript (AAM). The final published version (version of record) is available online via ELSEVIER at http://www.sciencedirect.com/science/article/pii/S0950423016304119?via%3Dihub. Please refer to any applicable terms of use of the publisher.

University of Bristol - Explore Bristol Research

General rights

This document is made available in accordance with publisher policies. Please cite only the published version using the reference above. Full terms of use are available:
http://www.bristol.ac.uk/pure/about/ebr-terms

Dynamic behaviour of direct spring loaded pressure relief valves connected to inlet piping: IV review and recommendations ☆

C.J. Hős[a], A.R. Champneys[b], K. Paul[c], M. McNeely[c]

[a] *Department of Hydrodynamic Systems, Budapest University of Technology and Economics, 1111 Budapest, Műegyetem rkp. 3. Budapest, Hungary*
[b] *Department of Engineering Mathematics, University of Bristol, Queen's Building Bristol BS8 1TR, UK*
[c] *Pentair Valves and Controls, 3950 Greenbriar Drive, Stafford, TX 77477, USA*

Abstract

Recent progress by a number of different groups and authors is reviewed on the stability properties of direct-spring pressure relief valves connected to pressure vessels with or without piping systems. Various different notions of stability and mechanisms for instability are revealed both in the case of gas and liquid service. It is stressed that it is not the valve itself that is stable or unstable, rather the harmful vibrations arise through interactions between the valve and its surroundings — the inlet piping, the reservoir, and any outlet piping. A distinction is drawn between underlying *instability mechanisms* and how these may be *triggered* during transient operations. The purpose of the work is to provide a coherent simplified account that will be of practical use for proposing new operational guidelines and mitigation strategies. Among these various mechanisms, oscillatory instability due to the interaction with a **quarter-wave** acoustic mode in the inlet piping is argued to be the most important to mitigate.

Keywords: pressure-relief valve, instability, acoustic waves, piping systems, quarter-wave, operational guidelines

☆ Short title: A review of pressure relief valves' dynamic behaviour

Contents

1 Introduction **4**
- 1.1 Current state of industry guidelines 4
- 1.2 Overview of main findings 9
- 1.3 Outline 9

2 Literature survey **10**
- 2.1 Experimental evidence 10
- 2.2 Modelling 11
- 2.3 Computational fluid dynamics 13

3 Mathematical modelling of the basic physics **14**
- 3.1 Valve mass flow rate 15
- 3.2 Reservoir dynamics 16
- 3.3 Valve dynamics 17
- 3.4 Pipeline dynamics 20
- 3.5 Reduced-order modelling 21

4 Primary instability types **24**
- 4.1 Chatter due to pipe pressure drop (3% instability) 24
- 4.2 Underdamped and oversized valves 25
- 4.3 Static instability — 'valve jumps' 28
- 4.4 Helmholtz instability 29
- 4.5 Quarter-wave instability 30

5 Transient events and triggering mechanisms **34**
- 5.1 Pressure surge on valve opening 34
- 5.2 Valve jump on opening and/or closing 36
- 5.3 Mid-lift instability - flutter 36
- 5.4 Flutter-to-chatter transition – grazing 37
- 5.5 Build-up of backpressure 37
- 5.6 Complex pipeline geometry and multi device installation . . . 38
- 5.7 Vortex shedding 39
- 5.8 Instability interactions 40

6 Summary and Recommendations **40**
- 6.1 Summary 40
- 6.2 Recommendations 42

6.2.1 Guidelines, standards and operating practice 42
6.2.2 Experimental validation 42
6.2.3 The role of CFD 42
6.2.4 Gases vs. liquids and multiphase flow 43
6.2.5 Validity of the 3 percent rule 44
6.2.6 Validity of the pressure surge criterion 44
6.2.7 Complex pipeline geometries 44

Appendix A Dimensionless parameters and equations 51

Appendix B Dimensionless parameters 52
Appendix B.1 Valve equation of motion 53
Appendix B.2 Reservoir pressure dynamics 53
Appendix B.3 Valve mass flow rate 54
Appendix B.4 Inertial pipe model 55

Appendix C Stability of linear models 55
Appendix C.1 Close-coupled valve (CCV model) 55
Appendix C.2 Helmholtz model 56

1. Introduction

Pressure relief valves (PRV) are the last line of defence for process plants in terms of over-pressure protection. If process supervision, either automatic supervisory control and data acquisition (SCADA) systems or human operators fail to cope with an unforeseen event, these valves are trusted to vent excess pressure and prevent an accident — typically the rupture of a pressure vessel. Several major disasters during the last thirty years have been attributed, at least in part, to improper system design or maintenance of such valves and their inlet/outlet systems. Details of many such accidents are available in reports from the US Chemical Safety Board CSB (2016).

To be concrete, we shall focus only on the standard topology of direct spring operated pressure relief valves (DSOPRV) commonly used in the oil and gas industry. We should stress though that parallels of the mechanisms of instability we describe through interaction between fluid flow and spring-mass systems occur in other industrial devices and sectors. Documented cases occur for example in nuclear engineering Galbally et al. (2015), steam power Yonezawa et al. (2012); Bolin and Engeda (2015), automotive fuel transmission Dazhuan et al. (2015) and hydraulic power transmission Mehrzad et al. (2015). Similar instabilities can also be present in other valve topologies e.g. Sverbilov et al. (2013); Yao et al. (2014), Venturi valves Zhang and Engeda (2003) and hydraulic dampers with blow-down Eyres et al. (2005a,b).

The primary aim of the current paper then is to provide a state-of-the-art overview on PRV instability in terms of modelling, classification of instability mechanisms, and how one might use this information to design specific mitigation strategies. A key goal is to demystify and simplify the literature in the light of recent studies that have proposed varying methods for analysis and prevention of instability. Thus we aim to enable simple design, operation and testing standards to be developed and and adopted. We focus on DSOPRVs that are connected to a pressure vessel with or without an inlet piping. Although not our primary focus, we also consider the presence of built-up backpressure but do not address any dynamics that might be associated with further downstream piping.

1.1. Current state of industry guidelines

Being aware of the primary importance of choosing and installing PRVs, industrial boards such as the American Petroleum Institute (API), the International Office of Standards (ISO), the American Institute of Chemical En-

gineers (AIChE) and the American Society of Mechanical Engineers (ASME) have issued guidelines on how to properly size and install these devices. Under steady-state conditions, the sizing, selection and installation of these valves is now well understood, see e.g. API-520 (2014). An experimental testing procedure, as detailed for example in ASME-PTC25 (2014), is also available to back this up.

The key difficulty in attempting to improve PRV safety though is that the performance of pressure relief systems is seriously limited by dynamic effects. Notably, it is well established that an open valve connected to downstream piping can be subject to different kinds of instabilities, variously known as chatter, flutter and rapid cycling. These instabilities typically cause the valve body to oscillate and periodically close, often at high frequency and with considerable force. Such oscillations in themselves are not necessarily a problem, but they can cause significant mechanical vibrations, and large upstream pressure waves (especially in liquids owing to the well-known water-hammer effect) that can cause system damage. For example, Smith and Burgess (2013) document at least four examples where chattering of relief valves was known to be a causal or contributory factor to plant damage. Furthermore, oscillations can severely restrict the valve's ability to vent at the required flow rate to relieve the over-pressure. Finally, the rapid oscillations typically cause wear and chafing in the valve itself that can increase its effective spring constant, thus compromising future pressure-relief events.

To date, guidelines have generally been insufficient in providing engineers with the necessary tools for *a priori* validation of the pressure-relief system design against instability. Up until about 2010, validating criteria were dominated by the *3 percent rule* (see e.g. Smith et al. (2011)). This rule stipulates a restriction on the the length of inlet line connecting the vessel to the valve by requiring that the frictional pressure drop from the tank to the valve should not exceed 3% percent of the *set pressure*, which, as we shall see in Sec. 4.1, might prevent one form of instability, which is typically not the most violent.

Starting in about 2010, the insufficiency of the 3% rule began to be recognised in a number of contemporaneous studies several presented at API meetings, many funded under the PERF programme, written up in later journal papers (e.g. Hős and Champneys (2012); Hős et al. (2014c); Izuchi (2010); Smith et al. (2011); Darby (2012); Aldeeb et al. (2014)) As a result, the latest revision of Section 7 of API-520 (2014) differentiates between PRV three different types of instability:

Cycling is defined as a low frequency (from a few fractions of a Hz to a few Hz) oscillation of the valve in which the pressure is quickly relieved upon opening the valve, causing it to close although pressure is continuing to build in the vessel, leading to a re-opening, and so on.

Flutter in contrast, is a typically higher-frequency oscillation, of the valve moving parts while it is open, without the valve making contact with its seat or upper stopper.

Chatter is a noisy, high-frequency (at the order of the valve's spring/mass system), high-energy oscillation of the valve including persistent impact between the valve and the seat.

More importantly, this distinction can be extended and further categorized by exactly which parts are oscillating, whether the valve motion is in synchrony or not with pressure waves in the valve's inlet pipe, and the precise triggering mechanism for the instability. Spelling out this further categorization is the main aim of this paper. To this list we shall add a fourth kind of instability:

Jump which is a sudden unexpected jump (up or down) in a valve's lift, causing a sudden change in discharge flow-rate.

Note that a valve jump need not strictly imply an instability, because valves are typically designed to *pop* open to a finite lift at their set pressure, and may also be deliberately designed to have jumps upon closing or at mid-lift.

Despite this recent progress, PRV test standards seem to be a few steps behind. For example ASME-PTC25 (2014) briefly suggests only that '*if the valve chatters, flutters, or does not reseat (as designed) satisfactorily, such action shall be recorded*'. Similarly, the European ISO-4216 (2014) mentions the word chatter only once; *The objective of the tests is to determine [...] the following characteristics of the valves [...]: absence of chatter, flutter, sticking and/or harmful vibration*'. Both of these standards appear to suggest that valve oscillation is an indication of a design or manufacturing flaw in the valve itself. Although poor design can indeed degrade valve performance (for example, through inappropriate body bowl shape), as we hope this survey paper will show, instability often occurs in a correctly designed valve if used under the wrong operating conditions.

Name	Description	Section	Guideline eq.
1. Inlet pressure loss	**Cycling** due to frictional and geometric losses within fluid flow in inlet piping. Causes low-frequency and low-amplitude chatter motion.	4.1	(8)
2. Oversizing/under-damping	**Cycling** or low-amplitude **chatter** due to insufficient damping and/or the valve venting at small portion of its capacity.	4.2	(9), (10)
3. Valve jumps	Static **jump** in valve lift due to negative effective valve stiffness.	4.3	(11)
4. Helmholtz instability	**Flutter** or **chatter** due to interaction between valve dynamics and the Helmholtz resonator formed by the tank plus the inlet piping.	4.4	(13) or (14)
5. Quarter-wave instability	**Flutter** or **chatter** due to *negative damping* of the fundamental "organ pipe" acoustic mode in an overly long inlet pipe	4.5	(15)

Table 1: Summary of the main types of instability and their description together with (third column) the subsection of Sec. 4 where the instability is described in more detail, and the equation number (fourth column) the necessary inequality guideline for *avoiding* the instability in question.

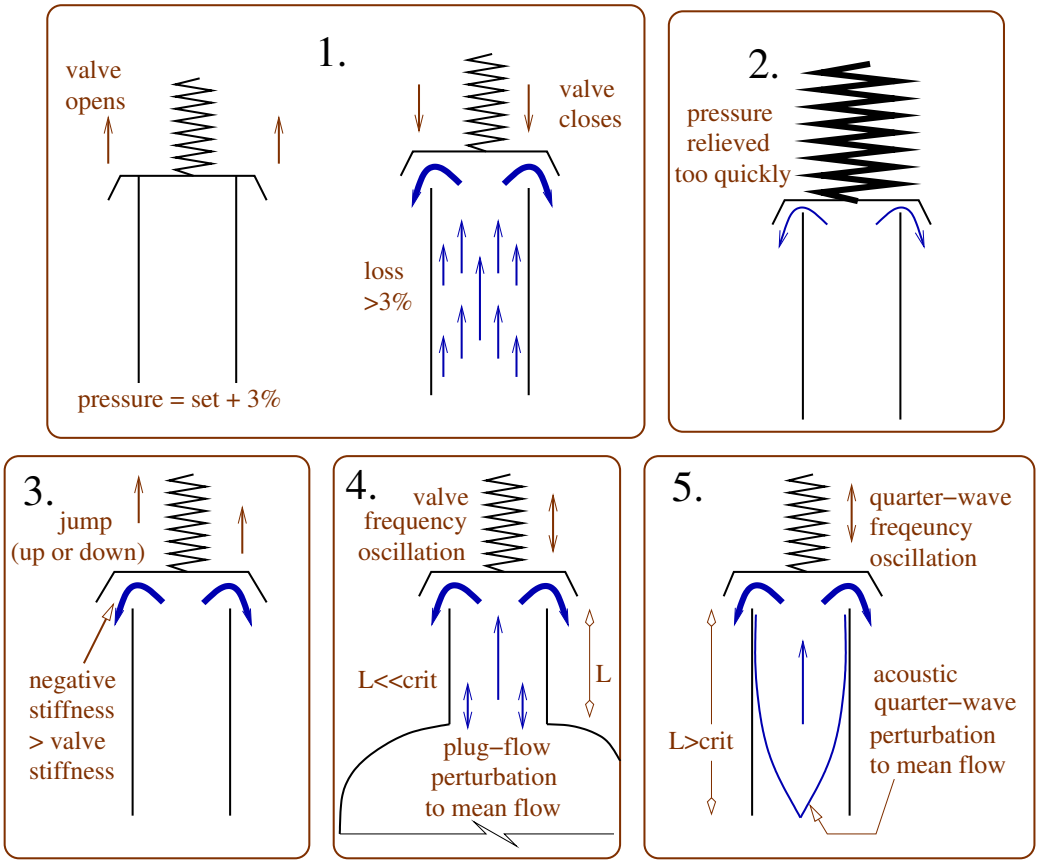

Figure 1: Schematic description of each type of instability listed in Table 1.

Name	Section	Associated instability
Pressure surge on valve opening	5.1	all
Valve jump on openning and/or closing	5.2	3.& 5. (or 4.)
Mid-lift valve jump	5.3	3. & 5. (or 4.)
Flutter to chatter transition	5.4	5. (or 4.), 2. or 1.
Build-up of backpressure	5.5	5.
Complex pipeline geometry	5.6	all
Vortex shedding	5.7	all

Table 2: Summary of possible instability triggering mechanisms for the instability including reference to section number where more detail, and, in the final column, the corresponding row of Table 1 of the associated instability.

1.2. Overview of main findings

The purpose of this paper is to summarise what is known about the origins of the various kinds of instability in DSOPRVs, how to differentiate between them and to propose criteria under which they can be avoided. The main types of instabilities are summarised in Table 1. A pictorial representation of each instability mechanism is given in Fig. 1.

We should stress throughout that one should *not* think of the valve as being either stable or unstable. Rather each form of instability is due to an interaction between the valve, the fluid being released and the vessel or piping system to which it is connected.

We should also stress the difference between a fundamental instability, and the transient event that might *trigger* the instability. Table 2 briefly lists possible triggering mechanisms.

A more complete scientific summary of our findings and a set of industry recommendations are delayed to the Conclusion of the paper.

1.3. Outline

The rest of the paper is organized as follows. In Section 2 we give an overview of the recent literature on valve instability, highlighting the state of the art both experimentally and in modelling and simulation. In order to discuss the origins of the different forms of instability, it is necessary to introduce standardized, simplified equations of motion for a valve interacting with

its environment. This forms the subject of Section 3. Then, Section 4 categorizes the different types of instability, explains their origins and suggests first principle guidelines that can prevent them. Section 5 goes on to further describe issues that can exacerbate instability, including transient triggered on opening or closing, dynamic jumps in valve lift, and the effect of backpressure. Finally, Section 6 concludes the work, gives summary recommendations and suggests avenues for future investigations.

2. Literature survey

Valve instability and chatter have long been known in the engineering science community, at least since the pioneering work of McCloy and McGuigan (1964), Funk (1964), Kasai (1968) and Green and Woods (1973). Literature reviews of scientific work up the about the year 2000 was carried out by Darby (2012) and until about 2010 by Hős et al. (2014c). Rather than repeat those surveys, we give here only an overview of recent developments, from the last 10 years or so.

2.1. Experimental evidence

One family of experimental-focussed papers include studies of in-situ measurements emerging from industrial case studies. A recent pertinent example is that of Galbally et al. (2015), who study the vibratory response of safety valves in the main lines within a boiling water reactor. Crucially, they find motion that represents a coupling between the *acoustic modes of the pipe* and the valve. Yonezawa et al. (2012) document instability occurring in a steam control valve with a flexible support, although in that case the flow direction is opposite to the usual PRV applications. Nevertheless, the authors' experiments confirm that the cause of instability is effectively *negative damping* of the valve head from the flow fluctuation in the pipe. In related work, Bolin and Engeda (2015) study instabilities of a Venturi-type control valve in a steam turbine.

A second family of studies are ones in which a specific test rig is designed solely for PRV instability measurements. In Aldeeb et al. (2014) the authors tested eighteen DSOPRVs from several manufacturers with inlet pipe lengths of 0, 2, 4, and 6 ft, and no discharge piping. Whether the valve was found to develop instability was reported, along with the opening time and the effect of the pressure rise rate. The pressure rise rate, had essentially no effect on the valve response. The valve opening time was found to vary between 20

and 50 ms at 50 psig and between 7 and 24 ms at 250 psig for 1E2, 2J3 and 3L4 valves. These numbers correspond to those reported by Singh (1983) who found valve opening times between 6 and 14 ms. More interestingly, it was also found that each of the 18 PRV's in the test program eventually became unstable. Even if a valve survived when attached to the 4ft inlet piping, none of them were found to be stable for the 6 ft inlet piping.

Another series of measurements were performed by the present authors in the test facility of Pentair between 2012 and 2015, which are well documented in Hős et al. (2014b, 2015) for both liquid and gas valves. These tests showed a similar tendency: longer inlet pipes cause more severe oscillations. Moreover, it *experiments* suggest that the critical pipe length (beyond which chatter occurs) depends on the valve flow rate similar to a square-root function meaning that *for small openings, the valve will always be unstable.* Whether the instability actually appears was found to depend on the *speed* with which the flow rate is increased (during opening) or decreased (during closure). These tests also suggest the root cause of instability upon opening (rarely encountered) and closing (more often encountered), that was reported in Aldeeb et al. (2014).

We also mention the liquid measurements reported in Bazsó and Hős (2013). There they also reveal an unstable range at low flow rates, which we shall refer to as *oversized valve* instability in what follows. This study also confirmed the presence of acoustic coupling between the inlet piping and the valve.

The effect of built-up backpressure was investigated experimentally by Chabane et al. (2009), backed-up by a computational study. They report the occurrence of chatter if backpressure is larger than 25-30% of the set pressure at which the valve opens. We also present new measurements of this effect in Sec. 5.5 below.

2.2. Modelling

In terms of modeling and providing design equations, Frommann and Friedel (1998) investigated two theories concerning vibrations in *pneumatic* systems: the "3% inlet pressure loss criterion" set by the API RP 520 and the so-called "pressure surge criterion", both of which define a critical pipe length above which oscillations will occur. With the help of experiments and numerical modelling they found that the 3% criterion is 'sufficient for a proper design', while the other is insufficient. It would appear that this

article was one of the main driving forces toward the wide reference to and adoption of the so-called three percent rule.

More recently Tamura et al. (2012a) used a lattice Boltzmann method to track the dynamics of a PRV. Interestingly, in the light of what follows, they found an instability associated with an acoustic resonance between the valve and the first quarter-wave associated with the piping. In fact, Misra et al. (2002) analysed an air-actuated control valve both numerically and with in-situ measurements and found also the same quarter-wave instability. Another documented example of the quarter-wave instability is given in Allison and Brun (2015), were the authors studied a PRV both experimentally and with numerical simulation. They also found that instability was most likely to occur with small openings of the valve and that the instability could potentially be removed by closing the PRV quickly enough.

Darby (2012) and Darby and Aldeeb (2014) presents an experimentally validated simulation model that is shown to capture the dynamics of a PRV with inlet piping. The method, apart from the details of the coupling with the fluid mechanics, essentially follow the same physics as presented in Sec. 3 below. Note that this method, like many others relies on the calculation of various "valve parameters" that are hard to quantify in practice. These parameters include a fluid damping coefficient ζ and the jet deflection angle θ_{avg}. Nevertheless, there is a nice match between the measured and simulated valve lifts.

We also mention here the evolution of the mathematical models developed by Hős and his co-workers. In Licskó et al. (2009), they built a simple system of three ordinary differential equations describing the valve motion and the pressure vessel for *hydraulic* systems, without inlet piping. After nondimensionalization they conducted both linear and non-linear stability analysis. The novelty of this work was the extensive use of the toolbox of nonlinear dynamics for conducting *qualitative and quantitative stability analysis*, beyond mere simulation, to explore the qualitatively different (stable/unstable) regimes of the parameter space. In a subsequent series of papers (Hős and Champneys (2012); Bazsó and Hős (2013); Hős et al. (2014b,a); Bazsó et al. (2014); Hős et al. (2015)), the authors further developed the models for *gas or liquid service* valves using 1D gas dynamics to represent transient motion in an inlet pipe. This also led, via the collocation method to a reduced order model. They reported a large number of experiments matching with model predictions. These papers also include clear evidence of instabilities associated with the first acoustic mode (a quarter-wave) of the pipeline system (see

Sec. 4.5) for details.

Similar results were previously found in the study by Izuchi at the Chiyoda Corporation in Japan, see e.g. Izuchi (2010). He constructed a model for the valve coupled to a finite-difference representation of the pipe dynamics. A good agreement is found with experimental results and a quadratic trend is found between the valve lift and minimum pipe length for quarter-wave instability (cf. (15) below).

2.3. Computational fluid dynamics

One significant consequence of Moore's law in the last decade or so has been the advances in and computational efficiency of computational fluid dynamics (CFD) such that it is now feasible to provide detailed simulations of fluid-structure interaction occurring inside a PRV. It is now possible to compute valve motion together with spatio-temporally highly resolved unsteady flow features including jets, shocks and transients effects formed during chatter. Nevertheless, it should be stressed that although CFD is the most advanced tool of describing fluid flow, it is designed to perform studies with stand-alone scenarios (valve geometry, excitation history, etc.) rather than quick parametric or qualitative studies. In a sense CFD is like a virtual experiment, and in our view does not circumvent the need for simpler low-order models to perform parameter studies, analytical approximation and qualitative interpretation.

Several recent articles in which the authors were able to reproduce various forms of valve instability using CFD include the works by Song et al. (2014); Srikanth and Bhasker (2009); Beune et al. (2012); Yonezawa et al. (2012); Bazsó and Hős (2012); Wu et al. (2015). CFD even allows the accurate predictions of two-phase situations, as in Dempster and Elmayyah (2013) or the analysis of other types of valves, see Qian et al. (2014). We also note that CFD can be useful to elucidate complex flow physics in the presence of reactive flows or combustion. There is also commercial software available for specific computation of opening and closing times of valves and their relation to instability e.g. Melham (2014a,b), see Sec. 5.1 for the principle behind this idea.

Another, less computationally expensive use of CFD, is to use it to calculate the elusive valve parameters (such as fluid damping coefficients, loss factors and jet angles), for static values of the valve lift. These can then be fed into the lower-order mathematical models. This approach has been

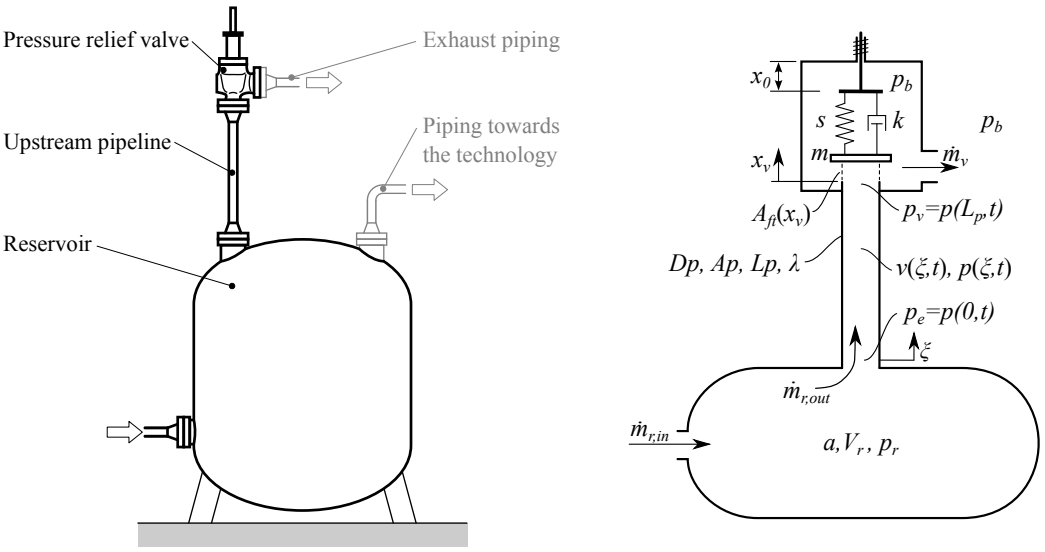

Figure 2: Left: typical PRV installation. Right: system sketch for mathematical modelling.

shown to effective to reproduce instabilities, see e.g. Moussou et al. (2010) or Erdődi and Hős (2015).

3. Mathematical modelling of the basic physics

In trying to understand the stability mechanisms of a PRV it is necessary to understand the basic physics of the device, what causes it to open and close, what causes instability and what transient effects can trigger instability. In order to present this in a scientific way, it is useful to introduce some basic equations of motion which also allow us to build *predictive* models. We study the standard PRV system depicted in Figure 2. Ignoring the complexities of the precise flow fields, there is basic agreement in the literature about the underlying equations of motion. We shall therefore review this material here, introducing some notation that will be of use in the rest of the paper. Readers who are less interested in the details of the models, may choose to skip to the next section.

The basic configuration studied throughout this work is depicted in Fig. 2; on the left-hand side a typical installation is shown while the sketch on the right defines the notation used in this paper. The mass flow entering the

reservoir (from some process) is $\dot{m}_{r,\text{in}}$, where the (stagnation, or static) pressure is p_r. The flow rate leaving the reservoir towards the upstream pipe is $\dot{m}_{\text{r,out}}$. The reservoir volume is V_r and the sonic velocity is denoted by a, both of which are assumed to be constant. The reservoir and the valve is connected with an upstream piping, in which $p(\xi, t)$ and $v(\xi, t)$ describes the velocity and pressure distribution, respectively, with t being the time and ξ being the axial coordinate along the pipe, such that $\xi = 0$ is the reservoir-end and $\xi = L_p$ is the valve-end of the pipe. Note that due to the inlet pressure drop, we have $p_r \neq p_e = p(0, t)$ (here 'e' stands for 'entering') in the general case. The diameter, cross-section, length and Darcy friction factor of the pipe are D_p, A_p, L_p and λ, respectively. The flow rate through the valve is denoted by $\dot{m}_v$ and, under steady-state assumptions, we have $\dot{m}_{r,\text{in}} = \dot{m}_{r,\text{out}} = \dot{m}_v$.

3.1. Valve mass flow rate

Steady-state flow through an orifice is well-understood for each of liquids (Melham (2014a); Misra et al. (2002), gases (Zucker and Biblarz (2002); Singh (1983); Darby (2012)) and multiphase flow (Leung (2004)).

In the case of valves in *liquid* service, the mass flow rate through the valve m_{out} can be written as

$$\dot{m}_{v,\text{liquid}} = C_d A_{\text{ft}}(x_v)\, c_1 \sqrt{(p_v - p_b)}, \tag{1}$$

where $c_1 = \sqrt{2\rho}$. C_d is the discharge coefficient, which depends on the geometry of the outlet, $A_{,\text{ft}}$ is the flow-through area of the valve, ρ is liquid density, p_v is the downstream pressure beneath the valve and p_b is the backpressure. There are several possible (more or less equivalent) definitions of flow-through area (different choices result in different C_d-values). The definition we shall use in the present study is based on the bore diameter D_{bore} (the narrowest section of the PRV upstream segment) and the valve lift $x_v(t)$ which is a dynamic quantity; i.e. $A_{ft} = D_{bore}\pi x_v$. Finally, note that if $\hat{p}_v = p_v - p_b$ denotes the *gauge pressure* above backpressure, we have

$$\dot{m}_{v,\text{liquid}} = C_d A_{\text{ft}}(x_v)\, c_1 \sqrt{\hat{p}_v}, \tag{2}$$

In the case of *gas* service, assuming choked flow, we have (see Zucrow and Hoffman (1976); Melham (2014a) for details)

$$\dot{m}_{\text{out,gas}} = C_d A_{ft}(x_v) c_1 \sqrt{p_v} \quad \text{with} \quad c_1 = \sqrt{\rho_v \gamma \left(\frac{2}{\gamma+1}\right)^{\frac{\gamma+1}{\gamma-1}}}, \tag{3}$$

where $\gamma = c_p/c_V$ is the ratio of specific heat capacities at constant pressure and volume. This is formally equivalent to (1) but now p_v is the *absolute* pressure at the upstream side so that the backpressure doesn't enter into the square root term.

In the case of multiphase flow, similar expressions can be derived that give the outflow as proportional to the valve lift times the square root of an appropriate pressure, see e.g. Leung (2004). In general though, it should be noted that the encapsulation of the exiting flow features into a single discharge coefficient C_d for a given fluid and geometry is an engineering simplification. In practice, as can be confirmed with CFD Misra et al. (2002); Bazsó and Hős (2012); Erdődi and Hős (2015), the 'coefficient' can be shown to a (typically quite weak) function of the valve opening, $C_d(x_v)$, which is relatively straightforward to determine experimentally. We should stress though that variation of C_d with x_v is *not* believed to be the primary cause behind any form of valve instability.

3.2. Reservoir dynamics

Pressure relief valves are by their nature connected to some kind of pressure vessel or tank, which we refer to generically as a reservoir of pressure. In order to derive the dynamics for the reservoir, we shall assume for simplicity that the pressure is rising via an inlet mass flow rate $\dot{m}_{r,in}$ that causes the pressure in the vessel to rise. The imbalance between this inflow and the outflow from the reservoir results in a change in the reservoir pressure, given by

$$\dot{p_r} = \frac{a^2}{V_r} \left(\dot{m}_{r,in} - \dot{m}_{r,out} \right). \tag{4}$$

Here V_r is the reservoir volume and a is the sonic velocity within the fluid, we have assumed for simplicity a constant reservoir temperature (which is a reasonable assumption over the time-scale of any valve instability). Note that in the absence of pipeline dynamics, the reservoir outflow $\dot{m}_{r,out}$ is equal to the flow $\dot{m}_v$ at the valve. However, there may be pressure losses due to either or both of pipe inlet pressure drop and frictional pressure losses inside the pipe.

Correct estimation of the sonic velocity is important in order to gain quantitatively correct instability prediction. For gases, we have $a^2 = \gamma R p_r$, where R stands for the specific gas constant. In the case of liquids though, any quantitative prediction of valve instability requires precise estimation of the sonic velocity, which should be carried out with care, see Wiley and

Streeter (1978); Hős et al. (2016). In theory the sonic velocity $a^2 = E/\rho$, with E being the bulk modulus of the liquid and ρ being density. The estimation of E requires careful consideration of the elasticity of the exit pipe of the reservoir, through its wall thickness, material properties and nature of its support mechanism. The fractional gas content of the liquid also significantly affects ρ and hence the observed value of a. In practice, it is recommended to estimate the sonic velocity through direct experimental measurements.

3.3. Valve dynamics

The rigid-body motion of the moving parts of the valve (including its body, shaft, spring, and, for balanced valves, bellows) can be regarded as a single degree-of-freedom mechanical oscillator, with equation of motion

$$m\ddot{x}_v + k\dot{x}_v + s\,(x_v - x_0) = F_{\text{fluid}} + F_{\text{gravitational}}. \tag{5}$$

Here, m stands for the mass of the moving parts for which it is common to include one third of the spring mass. This is reasoned by assuming linear velocity distribution along the spring, so that its kinetic energy is equivalent to that of a single rigid body with mass $m_{\text{spring}}/3$. The third term on the right-hand of (5) includes the spring stiffness s and the valve lift x_v relative to its precompression x_0.

The *mechanical* viscous damping coefficient k is usually designed to be as small as possible, because the various codes of practice stipulate that the valve should 'open unimpeded' when the pressure exceeds the valve's set value. However we should stress that valve motion can in practice be significantly damped due to *fluid-structure interaction* which is captured in the F_{fluid} term. The simplest explanation of equivalent mechanical damping would arise for example if the valve oscillates such as to transfer a portion of its kinetic energy to the generation of waves in the fluid. Note that such fluid effects can also, under certain circumstances, provide the equivalent of *negative damping*, which provides the most common underlying mechanism for valve instability (see Section 4). The key to understanding where such negative damping can arise from is to realise that if waves in the inlet piping are out of phase with the valve, then they can effective transfer energy back to the valve rather than visa versa.

These mechanical dynamics are balanced by gravitational and fluid forces. For a vertically mounted valve, the gravitational forces are equal to the weight

of the the moving parts, $F_{\text{gravitational}} = mg$. For most valves, these gravitational forces are very much smaller than the fluid or spring forces and can be ignored in any analysis.

Most of the difficulty in characterising the motion of PRV valves is to find a simple way to capture the fluid forces. As described in Singh (1983); Urata (1969); Song et al. (2013); Darby (2012); Bazsó and Hős (2012) or Allison and Brun (2015), the forces acting on the valve body can be characterized into three forms: force due to pressure distribution, force due to shear stress and impulse forces. In most cases, the shear stress can be neglected because of the small geometry associated with the pipe and hence the relative low Reynolds numbers involved. This leads to two terms

$$F_{\text{fluid}} = F_{\text{pressure difference}} + F_{\text{impulse}}.$$

Note that both of these terms depend closely on the valve's geometry and the flow field of the open valve. For example, in the case of a liquid service disk valve without a huddling chamber (so that the valve disk has the same area exposed to the fluid when open or closed) one can write

$$F_{\text{fluid}} = A_p\,(p_v - p_b) + \dot{m}_v|\mathbf{v}_{\text{in}}| + \dot{m}_v|\mathbf{v}_{\text{out}}|\cos\theta, \tag{6}$$

where A_p is the cross-sectional area of the valve's inlet pipe, $p_{v,b}$ are the upstream pressure and backpressure, respectively and $\mathbf{v}_{\text{in,out}}$ are the averaged inlet and outlet flow velocity vectors. The angle θ is the *jet angle*, as used in Darby (2012); Singh (1983) between the outlet flow and the valve inlet pipe. The case $\theta = 0$ represents a fully reactive jet, $0 < \theta < \pi/2$ is typical for disc valves and $\theta > \pi/2$ is typical for poppet valves. Note in general that θ depends on the valve lift and the mass flow rate and is difficult to measure in practice, or even to obtain via CFD computations.

Here we propose an alternative approach for capturing the fluid forces. To motivate this, let us start from (6) and use (1) to express $\dot{m}_v$ in terms of the valve lift x_v and the pressure difference $\sqrt{p_v - p_b}$. Note that the two final terms of (6) are quadratic in velocity. Hence, making use of (1) we can write

$$F_{\text{fluid}} = A_p(p_v - p_b)\left(1 + C_d^2 c_1^2 \frac{A_{\text{ft}}}{A_p}\left(1 + \frac{A_p}{A_{\text{ft}}}\cos\theta\right)\right) := A_p(p_v - p_b)\tilde{A}_{\text{eff}}(x_v), \tag{7}$$

where A_{ft} depends on x_v but A_p is constant. A similar equation can be derived for compressible fluids (gases). The above equation reflects to the

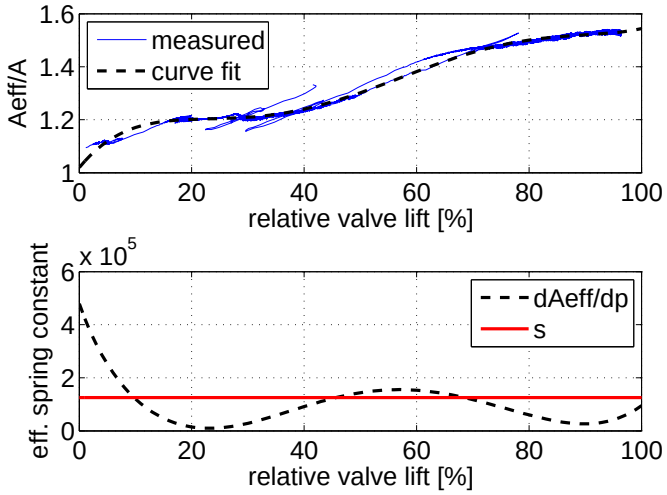

Figure 3: Upper panel: dynamic measurements of valve pressure and valve lift, and a fit to a single curve of effective area against lift. Lower panel: terms of effective spring constant, see Section 4.3 for details.

natural way of thinking of the fluid force as a pressure difference times an *effective area* A_{eff} Allison and Brun (2015); Moussou et al. (2010); Chabane et al. (2009); Hős et al. (2014c).

Using (7) we can think of $\tilde{A}_{\text{eff}}(x)$, the dimensionless effective-area-versus-lift curve, as an effective way to encapsulate a particular valve's operational characteristics. As it is demonstrated in e.g. Bazsó and Hős (2015), different valve geometries result in different effective area curves. Moreover, this curve us straightforward to obtain by CFD or, in the case of stable valve opening-closing scenario, via measurements. By definition, $\tilde{A}_{\text{eff}}(0) = 1$ when the valve is closed. Moreover, the blowdown of the valve (the difference between the opening and closing pressure) can be encapsulated in a small jump in this curve as $x \to 0$, which will also cause the valve to undergo a jump upon opening. Note that the effective-area concept is an approximation of the true physics but, unlike jet angles (see Darby (2012)), is particularly amenable to experimental measurement as shown in e.g. Figure 3.

3.4. Pipeline dynamics

The above equations with $\dot{m}_{r,out} = \dot{m}_v$ and $p_r = p_v$ would be sufficient to describe a valve connected directly to its reservoir. However, in practice upstream piping from the reservoir to the valve plays a central role in observed dynamical behaviour of pressure relief systems. This means that $\dot{m}_{r,out} \neq \dot{m}_v$ and $p_r \neq p_v$ and one needs to solve for fluid mechanical effects with the piping system. Physical phenomena that need to be captured within the piping include

1. pressure drop due to friction inside the pipe,
2. pressure drops due to the isentropic (ideal) acceleration of the fluid when exiting the reservoir and entering the pipe,
3. acoustic standing waves within the pipe fluid,
4. inertia of the fluid,
5. compressibility and temperature change (for gas and multiphase flow),
6. nonlinear, convective effects (if the pipe Mach number becomes a significant faction of unity),
7. shocks (for sufficiently large-amplitude waves in compressible flows) and
8. three-dimensional effects such as turbulent flow, vortex shedding or combustion.

Of course all these features can readily be captured using modern CFD techniques. However, CFD is only capable of simulating one particular unsteady pressure relief event at a time, and it is not well suited to make dynamic predictions nor to understand parameter trends. The key to understanding possible instability mechanisms and making quantitative predictions of instability trends is to use reduced-order modelling to capture just enough of the flow physics to accurately capture the phenomenon in question.

Apart from the final item in the above list, pipe flows are well approximated using one-dimensional unsteady fluid mechanics. Here one typically poses the equations of motion, the continuity equation and, if significant temperature variation is expected to occur, the energy equations. These represent a coupled system of partial differential equations (PDEs) that must be solved numerically e.g. with the help of the *method of characteristics* for liquids (see e.g. Wiley and Streeter (1978)) or the Lax-Wendroff technique (see Lax and Wendroff (1960); Press et al. (2007)) for gases. Mathematical models implementing these approaches are typically capable of predicting

full opening-closing cycles within engineering accuracy, however, special care must be devoted to properly implement the coupling to the reservoir and valve equations at the boundaries, taking care of possible shocks and inlet losses (see e.g. Hős et al. (2014b); Hős et al. (2016)).

3.5. Reduced-order modelling

In many cases, the pipeline dynamics can be captured through further reduction. An interesting approach is used in Misra et al. (2002); Burgess (2015), where the authors use a so-called impedance technique (IT) for capturing the pipeline dynamics. The technique is typically used for computing the hydraulic eigenfrequencies of pipeline system. It assumes small-amplitude periodic oscillations along the pipe and it is possible to connect the upstream and downstream pressure and velocity fluctuations via *linear algebraic* equations (transfer matrices). Although it is not clear how this technique can be generalized to predict valve instabilities, its capability of handling complex pipeline systems in a simple way is more than tempting.

In the case of a single straight inlet pipe, in Bazsó et al. (2015); Hős et al. (2014a) the present authors develop a reduced-order model that projects the full 1D fluid equations onto a finite number of standing wave modes in the pipe. Using a collocation method, one ends up with a pair of ordinary differential equations (ODEs) for the pressure and velocity amplitude of each mode. The first mode is the quarter-wave which as we highlighted in sec. 2, has been shown by many authors to be associated with valve instability. The advantage of this approach is not only that the PDEs are condensed into ODEs that can be solved with significantly less effort, but that the equations when coupled with the valve and valve and reservoir dynamics, allow for a full linear and nonlinear stability analysis.

The price of the simplification of the *quarter-wave model* is that it is a valid reduction of the full fluid dynamics only close to the onset of flutter, and it is not suitable for predicting fully transient behaviour. It is also not clear at present how to generalize this technique for complex geometries that involve many pipes with different diameters and complicated topology. In principle though it would be interesting to see how to combine this method of model reduction with the IT method.

Having said this, this quarter-wave model has allowed the *analytic* derivation of equation (15) below, which can be shown to provide a good match to both experiments and to full simulations, see Hős et al. (2015) for details.

In the rest of this paper, we will use the following models to capture the dynamics at instability. Each model has increased complexity and contains just enough information to capture the instability at hand. In each case we have checked that the instability is also present in higher-fidelity models and indeed in full scale CFD.

1. *Gas/Liquid dynamics model* (GDM/LDM): These models capture all the important features of 1D unsteady pipe flow: fluid inertia, compressibility, wave effects, friction, inlet pressure drop and convective terms. The governing equations and the numerical solution technique is available in Hős et al. (2015); Hős et al. (2016). This model is used mostly for quantitative validation purposes rather than qualitative analysis.
2. *Quarter-wave model* (QWM): This model assumes quarter standing waves in the pipeline, hence captures the acoustic coupling between the pipe and the valve. This instability type is described in Section 4.5. The governing equations and the model derivation is available in Hős et al. (2015); Hős et al. (2016).
3. *Helmholtz mode* (HeM): this model considers the piping between the reservoir and tank but assumes plug-like (constant density) flow in the pipes, hence includes the inertia and pipe friction of the fluid in the pipe but does not captures its compressibility or the waves. The model is given in Appendix C.2 and the corresponding Helmholtz instability is explained in Section 4.4.
4. *Close-coupled valve model* (CCVM): this model consists of a reservoir and a valve, the (upstream) piping is absent. The model captures the underdamped/oversized valve instability (Section 4.2) and the static instability (Section 4.3). The model is detailed in Appendix C.1.

The computations in the results in the following sections are all illustrated for a particular valve and geometry, whose parameters are given in Table 3, which represents a standard 2J3 valve with liquid trim. However, as the models we present are fully parametrized, the resulting formulae are general and can be used for any similar valve. For the sake of simplicity and generality, the various instability prediction formulae will be mostly given in terms of the dimensionless parameters listed in Table 4 whose precise definition is given in an Appendix.

Quantity	Symbol	SI	Imp.
Capacity	$\dot{m}_{\text{cap}}$	60.9 kg/s	30.45 lbm/s
Pipe length	L	0.91 m	3 feet
Pipe diameter (nom. inner)	D	52.5 mm	2.0 inch
Effective pressure diameter	D_{eff}	56.2 mm	2.2 inch
Seat diameter	D_{seat}	40.7 mm	1.6 inch
Reservoir volume	V	10.6 m^3	375 ft^3
Total effective moving mass	m	1.44 kg	3.18 lbm
Spring constant	s_v	101.6 kN/m	580 lbf/inch
Critical damping coeff.	k_{crit}	764 Ns/m	4.37 lbf s/m
Set pressure	p_{set}	8.3 bar	120 psig
Spring pre-compression	x_p	9.3 mm	0.368 inch
Maximum lift	x_{max}	11.9 mm	0.472 inch
Coefficient of discharge	C_d	0.93	0.93
Sonic velocity	a	890 m/s	2920 feet/s
Ambient pressure	p_0	1 bar	14.7 psi
Density of water	ρ	1000 kg/m^3	62.4 lbm/ft^3
Friction factor (Darcy)	λ	0.02	0.02

Table 3: Default parameter values (2J3 valve).

Quantity	Symbol	Definition	Value
Driving mass flow-rate	q	$\frac{\dot{m}_{\text{in}}}{\dot{m}_{\text{cap}}}$	0-1
Pipe length parameter	γ	(B.4)	0.273
Mass flow rate ratio	μ	(B.3)	0.0121
Spring pre-compression	δ	(B.1)	7.28
Reservoir-size parameter	β	(B.2)	0.171
Valve damping	$\hat{\kappa}$	(B.1)	0
Velocity-to-mass flow rate par.	σ	(B.3)	2.93
Velocity-to-sonic velocity par.	α	(B.4)	8.92
Friction factor	ϕ	(B.4)	0.000719
Reference pressure	p_{ref}	p_b	1 bar
Reference displacement	x_{ref}	$A_p p_b/s$	1.28 mm
Reference pipe length	L_{ref}	a/ω_v	3.35 m

Table 4: Reproduced from Hős et al. (2016) Key dimensionless parameters for DSOPRV attached to a straight inlet pipe in the case of liquids, their definition in terms of dimensional quantities and typical values for commercial 2J3 valves.

4. Primary instability types

In this section we explain in more detail the *primary* instability mechanisms present in DSOPRVs that were listed in Table 1 and shown schematically in Fig. 1. We also provide a simple design equations for ensuring the instability in question is not present. The detailed derivations of these conditions were either given in earlier work, to which we provide a reference, or are given in the Appendix to this paper.

4.1. Chatter due to pipe pressure drop (3% instability)

It is widely accepted that the pressure drop due to inlet pressure decrease and pipe friction can result in valve chatter. The fundamental mechanism is explained as follows (see Fig. 1 panel 1). Before the valve opens, the pressure at the two ends of the pipe ($p_e \approx p_r$ reservoir-end and p_v valve-end) are equal, up to the instant at which the valve opens. After the valve opens and flow in the pipe builds up, the valve-end pressure will be lower due to inlet pressure drop and friction pressure drop, i.e. $p_r > p_e > p_v$ and if it falls beneath the blowdown pressure, the valve will shut. At this point, as the flow rate vanishes, the reservoir pressure builds up again in the pipe and the whole process restarts.

Following the empirical work of Frommann and Friedel (1998), let p_{set} be the value of p_r at which the valve is set to open. Then the 3% requirement stipulated by API-520 (2014) is that at the point of opening, taking all pressure loss into account, we require

$$(p_v - p_r)|_{\text{valveopen}} < 0.03 p_{\text{set}}. \tag{8}$$

Note that it is possible to capture the rapid cycling associated with the 3% using any mathematical model that at least includes pipe frictional losses. Fig. 4 shows how the effect can be captured in the Helmholtz model with added pipe friction and a non-trivial effective area curve. Here the valve opened in a stable manner and a pressure level developed in the reservoir that was capable of keeping the valve pressure above the set pressure, despite the presence of frictional pressure loss. We had to add a non-zero effective area curve, resulting in large and sudden valve openings in order to obtain the result shown in Figure 4.

This result indicates that upstream pressure loss exceeding the blowdown pressure, is not sufficient in itself to cause unwanted oscillations, it only might do so depending on the precise valve geometry.

4.2. Underdamped and oversized valves

An oversized valve – i.e. a valve venting only a portion of its capacity – will self-oscillate if connected to a reservoir, even without inlet piping. It must not be forgotten that for most of the reactive PRVs, i.e. the when jet deflection angle is larger than 90 degrees, the fluid momentum force adds to the pressure force and, for small openings, this extra momentum force is not sufficient to keep the valve open. Hence, for low flow rates the valve will indulge into an opening/closing cycle resulting in low-frequency cycling behaviour. There are many reports of valves being unstable at small openings, e.g. Allison and Brun (2015); Hős and Champneys (2012); Bazsó and Hős (2013).

We shall now employ our simplest model, i.e. the CCV model, whose governing equations can be found in Sec. Appendix C.1, with the assumption of $\tilde{A}_{\text{eff}} \equiv 1$. Standard linear stability analysis shows that the damping needed to obtain stable valve motion is

$$\hat{\kappa} > \hat{\kappa}_{crit} = \frac{q}{y_{1,e}^2 \beta \mu^2 \sigma^2} \left(-\Delta + \sqrt{\Delta^2 + \left(1 + \frac{y_{1,e}^2 \beta^2 \mu^4 \sigma^4}{4q^2} \right)^2} \right) \tag{9}$$

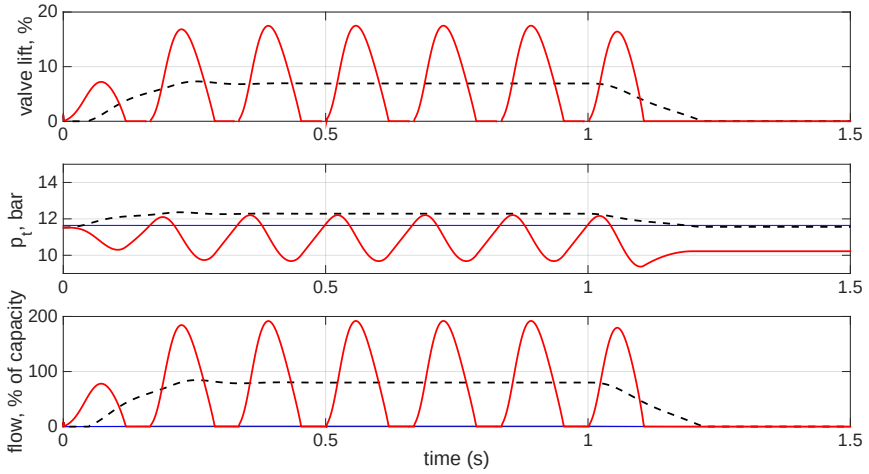

Figure 4: Demonstration of rapid cycling due frictional pressure drop, using the Helmholtz model with parameter values in Table 4 except that $\delta = 11.6$, $\mu = 0.121$, $\varphi = 0$ and $\gamma = 0.1$ and a cubic non-trivial effective area curve was used. The dashed line shows what happens when no frictional loss is included

where

$$\Delta = 1 + \frac{y_{1,e}^4 \beta^2 \mu^4 \sigma^4}{4q^2}$$

and $y_{1,e}$ is the valve equilibrium for a given flow rate q. For small flow rates, upon making use of the approximate formula (C.2) for $y_{1,e}$, (9) can be rewritten as

$$\hat{\kappa} > \hat{\kappa}|_{\text{small q}} = \beta \left(\sqrt{\delta}\mu\sigma + q\frac{1}{2\delta}\left(1 - \beta^2\delta\mu^2\sigma^2\right) \right) + (\mathcal{O})(q^2). \qquad (10)$$

Note that the $\hat{\kappa}$ in this equation needn't necessarily be viscous mechanical damping of the valve spring, but is mostly likely to be dominated by the effective fluid damping within F_{fluid} (6).

Equation (10) reveals that for large reservoirs (i.e. for small β) then the amount of damping required for stability is small, although this required damping increases slightly with flow rate q if $\beta^2\delta\mu^2\sigma^2 < 1$. If however the β is large (for a small reservoir) then a larger amount of damping is required to avoid instability. Moreover, if $\beta^2\delta\mu^2\sigma^2 > 1$ this this required damping is maximised for small flow rates q (i.e. for small valve lifts). Typically such

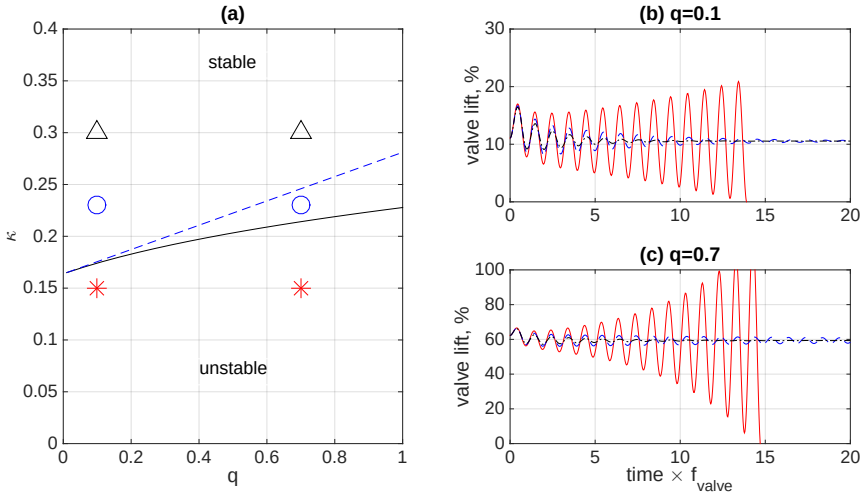

Figure 5: Underdamped instability: linear stability (left) and time histories (right) of the CCV system. Parameter values are the same as in Table 4, but $\delta = 7.28$ and $\beta = 1.71$ (a ten times smaller reservoir).

damping levels are not present, and this leads to an instability for small valve openings. The reservoir being too small is an indication of the choice of valve being too large for the task at hand, hence this is known as an oversized valved. Note that valve sizing is a key part of any installation process of any relief valve in practice.

Figure 5 depicts the stability diagram (panel (a)) and some time histories (panel (b) and (c)). In panel (a), the solid line gives the accurate stability boundary (9) while the dashed line is the approximate criteria (10). On the right-hand side, the solid red line depicts the time histories at the unstable $\kappa = 1.5$ values (red asterisk in panel (a)) while the blue dashed and black dash-line graphs are the simulation results at the parameter values denoted by the blue circles and black triangles in panel (a). Note that in the case of the time histories (b) and (c), the time was rescaled by the eigenfrequency of the valve (i.e. one valve oscillation lasts for unit time) and the period of the appearing oscillation is unity in this scale meaning the frequency of the oscillation coincides with the valve eigenfrequency.

4.3. Static instability — 'valve jumps'

The simplest instability type, whose occurrence requires neither inlet piping, nor pressure vessel dynamics is the static instability of the valve, which, instead of causing oscillations, will result in valve jumps. To describe such an instability, we assume no inlet piping, neglect the inlet pressure drop, hence $p_v = p_r$. We also consider large vessels with constant pressure. Under these assumptions, the valve motion is described by (5) with constant valve (reservoir) pressure p_v and also constant backpressure p_b.

Now we think of the pressure drop through the valve $\Delta p = p_b - p_r$ as a control parameter. For different values of Δp, the valve equilibrium x_e will also be different and solves $s\,(x_e - x_0) = A_{\text{eff}}(x_e)\Delta p$. Next, we expand the effective area curve into Taylor series around x_e giving

$$A_{\text{eff}}(x)|_{x=x_e} = A_{\text{eff}}(x_e) + \left.\frac{\mathrm{d}A_{\text{eff}}}{\mathrm{d}x}\right|_{x=x_e} (x - x_e) + \text{h.o.t.}$$

Upon introducing a new variable $y = x - x_e$ that measures the deviation from the equilibrium position, the equation of motion (5) becomes

$$m\ddot{y} + ky + (s - A'_{\text{eff}}(x_e)\Delta p)\, y = 0.$$

Hence we see that the *slope* of the effective area curve modifies the spring stiffness and the 'effective stifness' has to be positive, i.e.

$$s_{\text{eff}} = s - A'_{\text{eff}}(x_e)\Delta p > 0 \tag{11}$$

in order to have a *statically* stable equilibrium. If the pressure difference is large or the effective area curve is too steep, the effective spring stiffness becomes negative, which typically happens at small openings and results in 'valve jumps', i.e. sudden change in the valve lift during opening or closing. We shall emphasise that this kind of instability does not cause chatter or flutter *per se*.

This result is consistent with the findings reported in Moussou et al. (2010), where, based on a similar model, the authors conclude that the stability condition is that the slope of the spring force must be larger than the slope of the fluid force. Moreover, experimental evidence of these valve jumps is also reported. Bazsó and Hős (2012) also reports on the importance of the effective area curve shape and provides examples of such curves for different closing body geometries. Finally, we refer to Hős et al. (2014) for both analytical considerations and experimental results.

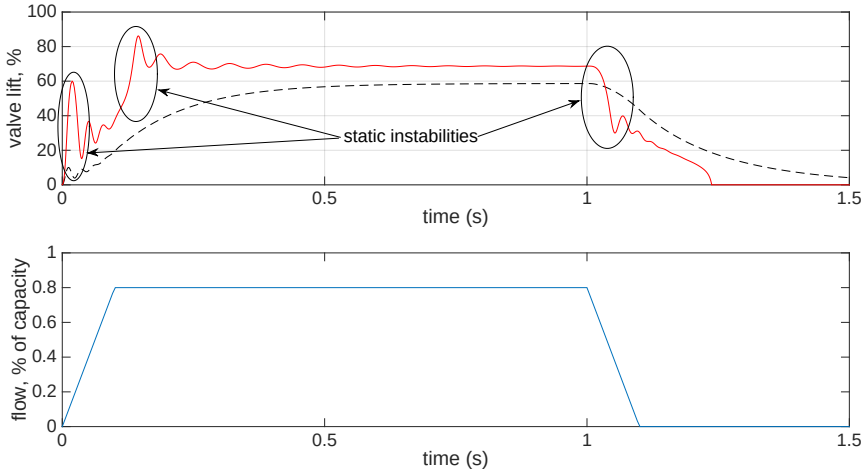

Figure 6: Demonstration of static instability, i.e. valve jumps with the help of the CCV system C.1. Upper panel: valve lift in the case of constant effective area (dashed line) and with realistic effective area curve, see Figure 3. Lower panel: prescribed reservoir inlet flow rate time history vs. time. Parameter values: $\delta = 11.64$, $\mu = 0.01212$.

4.4. Helmholtz instability

It is well-known that pipes connected to a vessel form a mass-spring-like oscillatory system, whose eigenfrequency is given by (see e.g. Chanaud (1994) for details)

$$\omega_H = a\sqrt{\frac{A_p}{V_r L_p}}, \tag{12}$$

where a is the sonic velocity, V_r is the vessel volume, A_p and L_p are the pipe cross section and length, respectively. It seems natural to assume that the valve and the Helmholtz resonator (pipe and reservoir) might come into resonance. Indeed, in Hős et al. (2016) it was shown that there is a form of instability, when the pressure fluctuation in the vessel is compensated by the quarter-wave in such a way that although the pressure in the pipe oscillates, the fluid moves in a plug-like way such that the pressure is approximately constant at the valve-end of the pipe. After performing the necessary computations, we found in Hős et al. (2016) that the critical dimensionless pipe

length γ for instability and frequency of motion are given by

$$\gamma < \gamma_c \approx \frac{\pi\beta\mu}{2\sqrt{2}\alpha}, \qquad \omega_v^2 = \frac{\pi}{2\sqrt{2}}\omega_H^2. \tag{13}$$

In Appendix C.2 below, we present a simpler calculation that captures the instability accurately without complicating the model with wave effects or liquid/gas compressibility. This system models the pipe via the *unsteady* Bernoulli equation, which is coupled to the reservoir and valve equation. Standard linear stability analysis reveals an instability with frequency $\omega = \omega_H$ that occurs provided

$$\gamma < \beta\frac{\mu}{\alpha} \quad \text{or, equivalently,} \quad L_p > \frac{a^2 A_{pipe}}{V_r}\frac{1}{\omega_v^2}. \tag{14}$$

Another way of viewing this is that for stable valve opening, the valve eigenfrequency ω_v must be *above* the Helmholtz frequency.

Note the difference between (both the frequencies and critical γ's) for two formulae (13) and (14) is a factor of only $\sqrt{\pi/2/\sqrt{2}} \approx 1.054$. We speculate that this discrepancy is due to the former criterion being derived from the quarter-wave model, which approximates the flow by an assumed velocity distribution inside the pipe rather than plug-like flow.

It should also be noted that for industry sized vessels and inlet pipes the Helmholtz frequency is typically much less than a few Hertz while the order of magnitude of the valve eigenfrequency is 10-100 Hz, hence, this kind of instability is not expected to be an issue in practice. Nevertheless, Smith et al. (2011) mention Helmholtz resonators and cavity resonance as a potential source of frequency matching leading to instability.

4.5. Quarter-wave instability

The presence of inlet piping gives rise to the formation of acoustic standing waves, which can couple with the valve dynamics and result in flutter and chatter. Typically, one encounters the first, quarter-wave, harmonic of the pipe — that is a standing wave of wavelength of four times the pipe length. Examples of such vibrations can be found in Allison and Brun (2015), where the authors found that the quarter-wave frequency to dominate valve oscillation. Similarly, in Misra et al. (2002) the quarter-wave eigenfrequency of the downstream piping was found to match with the observed vibration

frequency. In Tamura et al. (2012a) a standing quarter-wave was found numerically in the stub pipe of several relief valves during the oscillations. We also point to our previous work Hős et al. (2014); Hős et al. (2015); Hős et al. (2016)) where, besides mathematical modelling, a large amount of experimental evidence was provided for the presence of quarter-wave instabilities in both liquid and gas service.

As described in Hős et al. (2015), the main mechanism behind this kind of instability is the coupling between the valve motion and the first acoustic eigenmode of the inlet piping. Rather than looking for triggering mechanisms *per se*, the analysis considers inherent instability by assuming that a valve is at an intermediate lift *equilibrium* position (x_e) under steady-state operating conditions, and asks whether such an equilibrium is stable. In other words, if any small perturbation is introduced to the system, will it decay so that the valve returns to equilibrium, or will it grow into large amplitude motion. In the case of the quarter-wave instability, any such large-amplitude motion be in the form of a coupled oscillation between the valve and the acoustic mode, predominately at the acoustic mode frequency.

The details of the calculation of the quarter-wave instability criteria are given in Hős et al. (2015). Roughly speaking, the analysis shows that the valve acts as a damper on the pipeline acoustic dynamics and the phase shift between the valve and the pipeline motion determines whether this damping is positive or negative. It is then possible to derive an approximate analytical expression for the flow rate at which this *negative damping* first arises. Specifically, we find that the flow rate

$$q > 2\frac{(1+\delta)^{3/2}}{\omega_1^2 - 1}\mu\sigma, \quad \text{with} \quad \omega_1 = \frac{\pi}{2\gamma}. \tag{15}$$

The formula (15) For a given dimensionless pipe length γ, this formula formula provides *a critical flow rate beyond which the valve will be stable* or, to put it differently, for a flow rate q *there exists a critical pipe length, beyond which the valve is unstable*. We found the above formula to be particularly accurate in the case of liquid service valves Hős et al. (2016). If the valve is in gas service, the above formula can be still used provided that the gas properties (notably density and sonic velocity) are evaluated at set pressure. In both the liquid and gas cases, the formula was found to capture the critical pipe length with reasonable accuracy, see the experimental and simulation results reported in Hős et al. (2015); Hős et al. (2016). These results and

notably, the mechanism behind it is also consistent with the findings of Izuchi (2010). Moussou et al. (2010) also explains the emergence of instability — based on experimental and analytical computations — using the idea of principle of negative damping.

It should be emphasized that the formula (15) must be handled with great care as it results from a simplified analysis that neglects effects that may be important in a particular implementation, such as inlet pressure drop and pipe friction, non-trivial effective-area-versus-lift relationships, variation in effective inlet pipe diameter at the valve inlet, backpressure, high Mach-number or Reynolds-number effects, etc. Nevertheless the principles leading to the formula (15) can readily be adapted to deal with these additional effects.

Another thing to note is that while the formula 15 appears to capture the mechanism of instability onst, it does not necessarily describe the post-instability dynamics. In particular, it can be hard experimentally to observe unstable oscillations that are dominated by the quarter-wave frequency itself is hard to find experimentally. According to the experience of the authors and the experiments published in Hős et al. (2014); Hős et al. (2015); Hős et al. (2016), once the oscillation is born, it grows quickly and goes from flutter to chatter. In fact, we showed in theory in Hős et al. (2016) that for the case of liquids, just beyond the threshold for instability, the dynamics will jump immediately into chatter. This is because limit cycle motion associated with finite amplitude flutter in this case is unstable (a so-called sub-critical bifurcation). In contrast, for gas-service valves, a steady flutter limit-cycle motion may be observed, but its amplitude is shown to grow quickly with increased flow rate, such that impacting chattering motion ensues. Such chattering involves violent impact of the valve with its seat, which results in higher often broad-band frequency content.

Figure 7 shows experimental results for a 2J3 valve in liquid service. We have plotted two different analytical criteria that have been used to predict instability thresholds. The solid line depicts the analytical estimate of the quarter-wave model (QWM), specifically equation (15). The dashed line represents the 3% rule (8). Notice how the 3% rule has exactly the wrong trend. Many unstable points (for low flow rates in particular) are beneath this curve. In contrast, the quarter-wave instability prediction provides a good explanation of the trends in the experimental data.

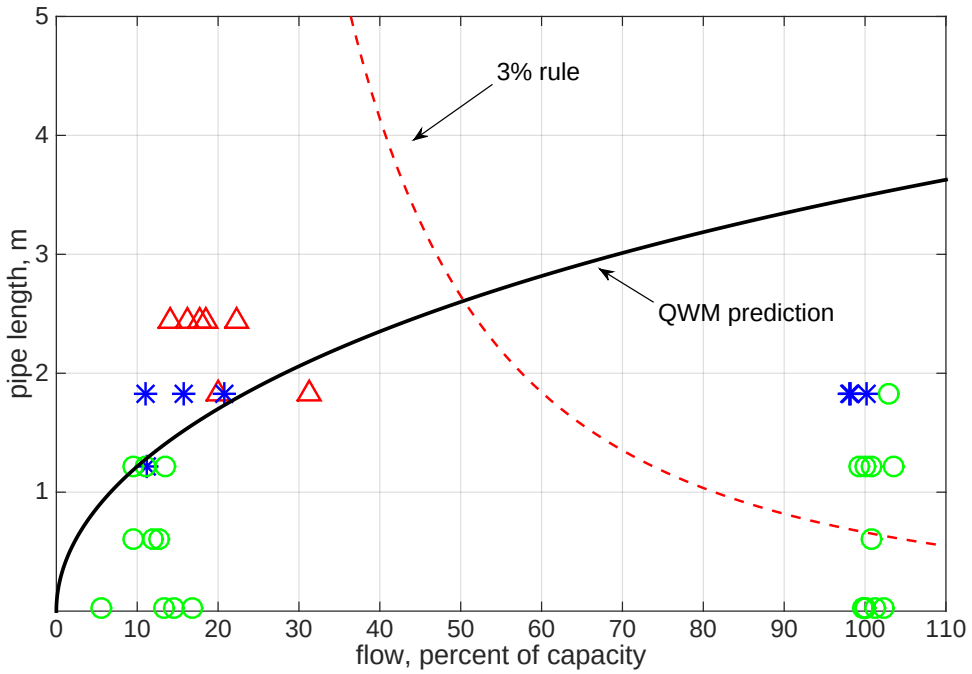

Figure 7: 2J3 test results, reproduced from Hős et al. (2016) with permission. Different symbols represent the measurement points: (red, colour online) triangles show test runs that were fully unstable, (blue) asterisks are unstable on closing, (green) circles are fully stable. Two theoretical predictions are presented for completeness, the (red) dashed line shows the critical pipe length corresponding to the 3% rule, and the (black) solid line is the analytical prediction for the quarter-wave instability. In both cases, the stability criterion is that the measurements should lie beneath these curves. Note that with the 2.5 m pipe length, it was impossible to reach the capacity flow rate due to the heavy oscillations.

5. Transient events and triggering mechanisms

One of the most important things when understanding the propensity of a PRV system to develop instability is to distinguish between the inherent reasons why the system is unstable for a certain valve lift, and what may be the transient triggering mechanism for the instability. In the previous section we reviewed the inherent instability mechanisms. In contrast, this section seeks to review and explain the transient mechanisms that can trigger or exacerbate an instability.

5.1. Pressure surge on valve opening

Dating back to Singh (1982) and the later works of Cremers et al. (2001), Melham (2012) and Darby (2012), the so-called pressure surge criteria is often used to predict whether the opening of the valve will trigger chatter upon valve opening opening. This criterion, which is commonly included as part of design guidelines, focuses on the transient dynamics during valve opening in a simplified, quasi-steady manner. Essentially, it is postulated that according to Cremers et al. (2001) - the '*valve is expected to operate in a stable manner, resp., not to chatter if twice the transmission line time t_w of the expansion wave in the inlet pipe, generated by the abrupt valve opening, is shorter than the total opening time t_{open} of the valve*'.

There are several variants of the actual design equation, we shall use the notation in Melham (2012). To compute the pressure decay at the valve due to the fluid hammer effect Δp_{wave}, we make use of the Joukowsky theory (see e.g. Wylie and Streeter (1993) for details), i.e. assuming linear change in the pressure, velocity change Δv in time interval t_{open} causes a pressure drop given by

$$\frac{\Delta p_{\text{wave}}}{\Delta p_{\text{Jouk}}} = \frac{t_w}{t_{\text{open}}} \quad \text{with} \quad t_w = \frac{2L}{a} \quad \text{and} \quad \Delta p_{\text{Jouk}} = \rho a \Delta v = a\frac{\dot{m}}{A_p} \tag{16}$$

provided that $t_{\text{open}} > t_w$. However, if the valve opening is hydraulically quick (i.e. $t_{\text{open}} < t_w$), we have $\Delta p_{\text{wave}} = \Delta p_{\text{Jouk}}$. Another source of pressure decay is due to the fact the the fluid accelerates ($\Delta p_{\text{inertia}}$) and hence, the a portion of the stagnation pressure beneath the earlier closed valve is lost:

$$\Delta p_{\text{inertia}} = \frac{\rho}{2}\left(\Delta v\right)^2 = \tau^2 \frac{\dot{m}^2}{2\rho A_p^2} \quad \text{width} \quad \tau = \min\left(\frac{t_w}{t_{\text{open}}}, 1\right) \tag{17}$$

The third effect decreasing the pressure beneath the seat is again pipe friction, which we shall simply denote by Δp_{fric} and should be straightforward to compute. Finally, at the end of the opening process, the estimated pressure beneath the valve disc is

$$p_v|_{t=t_{\text{open}}} := p_{v,\text{min}} = p_{\text{set}} - \Delta p_{\text{wave}} - \Delta p_{\text{inertia}} - \Delta p_{\text{fric}}. \tag{18}$$

The design process process proposed by Melham (2012) is to ensuring that this minimum valve pressure $p_{v,\text{min}}$ is above some user-defined safety level, typically the reseat pressure (or, possibly, the initial closure pressure, see Singh (1983)).

Although the pressure surge criteria is tempting due to its simplicity, it should be noted that its derivation would appear to be somewhat *ad hoc* and, to the best of our knowledge, there is no systematic computational or experimental study that shows its validity as a predictor of an instability threshold. One particular simplification, given the typically complex geometry of PRVs, is that the inertial term in (17) is a gross approximation to the true large-amplitude transient fluid dynamics involved. Also, given this large transient, the assumption that frictional loss can be computed by means of steady-state assumptions probably overestimates the actual value (nevertheless, it is a conservative estimate on the 'safe side'). Also, if the reflected wave reaches the valve again during the opening process, the Joukowsky estimate (16) gives limited accuracy. At least in the case of liquid-service valves such reflected waves can lead to significant instantaneous jumps in pressure at the valve due to the well-known *water hammer* phenomenon. For example, in Hős et al. (2016), such pressure peaks were found to be several times that of the set pressure. It is interesting to note that Frommann and Friedel (1998) were unable to measure the reflection of the first expansion wave as a compression wave due to the area contraction in front of the vessel nozzle. The same authors state — based on their experiments — that the pressure surge criterion 'may be insufficient' to describe the process during opening, especially when using an inlet pipe that has a wider diameter than that of the valve.

Another weakness of the formula (17) is that it requires information on the valve opening time t_{open}, which is not readily available for commercial valves. Also, t_{open} is not really a valve parameter as such, but is an approximation of a dynamically measurable quantity that also depends on fluid properties and flow conditions. Nevertheless, one can make broad order-of-magnitude

estimations, and both Melham (2012) and Singh (1983) provide formulae or data for specific valves.

5.2. Valve jump on opening and/or closing

In many experiments, authors report that the valve is unstable during opening or closing, but stable for the full-lift regime. It also often experienced that closing is less stable than opening. Figure 7 together with the valve jump instability explains these phenomena. During a full opening and closing cycle, one moves vertically in the Figure, along a constant pipe length value: we start off at $q = 0$ (closed valve), move to the right up to $q = 100\%$ and then, during closing, we move to the left back to $q = 0$. For example, take a pipe length of 2 meters. This means that up to approx. 30% of the flow rate, the valve will be unstable but then stabilizes for larger flow rates. This already explains why a valve is unstable only at small openings.

One can also readily explain why closing instabilities are more common than opening ones. Valve opening is a 'fast' transient, which, due to the static instability, occurs over a short time window that does not allow oscillations to develop. However, valve closing is a slower process – see Figure 6 – which allows slow passage into the q-range for which the system is unstable to quarter-wave oscillations. In other words, during opening, the left-to-right sweep in the stability map of Figure 7 is a fast motion and the valve 'jumps over' the unstable region of low flow rates. The backward (closure) right-to-left motion is slow, which allows the formation of the quarter-wave instability at low openings.

5.3. Mid-lift instability - flutter

Mid-lift instability can be experienced because of a combination of valve jump instability and the quarterwave. Upon either increase or decrease of flow rate (equivalently, the reservoir pressure), an otherwise stable valve, can reach a lift-value at which it jumps to an unstable point that is unstable to the quarter-wave oscillations. This can lead to flutter, which may rapidly transition into chatter. Note that such transitions can exhibit hysteresis. That is, once oscillations have set in, reversal of the change in flow conditions that lead to the instability would not be sufficient to quench the undesired motion. It is also possible that due to the larger spring pre-precompression and set pressure, there exists no stable equilibrium in the entire lift range, resulting in a continuous, low-frequency oscillation. Figure 8 depicts a simulation similar to Figure 6 with increased set pressure ($\delta = 13.1$). Note that

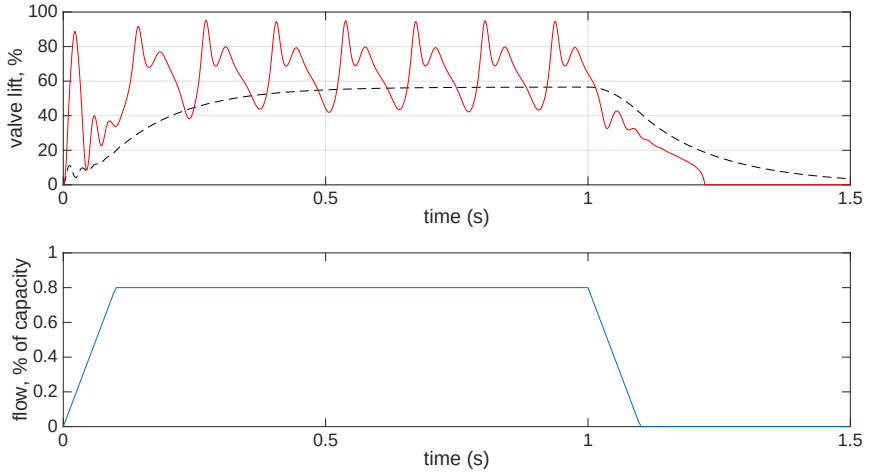

Figure 8: Mid-lift flutter due to effective area curve with high set pressure: same as Figure 6 but with $\delta = 13.1$, obtained with the CCV system C.1. Upper panel: valve lift in the case of constant effective area (dashed line) and with realistic effective area curve, see Figure 3. Lower panel: prescribed reservoir inlet flow rate time history vs. time.

(11) predicts this trend clearly: the higher the set pressure (here, Δp), the smaller the effective spring stiffness becomes.

5.4. Flutter-to-chatter transition – grazing

The distinction between flutter and chatter can represent the difference between undesirable but safe and truly damaging oscillation. Typically, a quarter-wave instability causes flutter which, especially for higher set pressures and for liquids, rapidly leads into chatter. As shown theoretically in Hős and Champneys (2012); Bazsó et al. (2014) the transition point between flutter and chatter can be understood in terms of where a flutter cycle first *grazes* with the valve seat. Those references show that grazing can be responsible for the onset of either chaotic or multi-frequency dynamics. Typically there is much more energy dissipated in such impacting motion.

5.5. Build-up of backpressure

Several studies report on instability appearing with increased backpressure. Chabane et al. (2009) studied the effect of built up backpressure both experimentally and with the aid of CFD. They report on the occurrence of

chatter if backpressure is larger than 25-30% of backpressure. Singh (1983) also finds a 'slight instability' due to backpressure, which is formed during valve closure. Smith et al. (2011) and the references therein confirm that increased backpressure increases the likelihood of chatter. With the help of numerical simulation Chabane et al. (2009) arrives at the conclusion that backpressure degrades the resistance of PRVs against chatter.

We report here on a series of new experimental results that were performed in the Pentair test facility with a standard 2J3 valve both in liquid and gas service. The experimental details were the same as those reported in Hős et al. (2014b); Hős et al. (2016) with inlet piping varied between 0 and 48 inches. In addition an outlet pipe was fitted to the valve, whose length was varied between 0 and 230 inches. The main effect of the outlet piping was to add backpressure.

The results can be summarised as follows. First and foremost, a valve-inlet-pipe system that was unstable without outlet piping was never found to be stabilized by the addition of outlet piping. This is hardly surprising given the strong indication in the literature that additional backpressure has a destabilizing influence. For a system that could sometimes be unstable, depending on the mass flow rate, little difference was seen upon increasing outlet pipe length. There was however a mild effect that pipes with increased outline pipe length would become unstable for slightly lower flow rates. We also tested the same valve with bellows but did not experience any striking difference. The main outcome of these experiments was the conclusion that although increased backpressure mildly degrades the stability properties, the main parameter that determines the flow rate at which instability will occur is the inlet pipe length.

5.6. Complex pipeline geometry and multi device installation

Most of the theoretical and numerical studies referenced, assume the inlet piping to be a simple straight pipe with constant diameter, which is rarely the case in real-life systems. The inlet (and the outlet) piping often includes elbows, junctions, etc. and it is not clear how these elements influence the onset of flutter and chatter. Moreover, to the best of the authors' knowledge, there is no systematic agreement as to whether transient valve oscillations are amplified or suppressed by these additional geometric complexities. On one hand, these elements add damping and loss to the system, which might help to break-up acoustic modes that might otherwise lead to a quarter-wave instability. On the other hand, they also introduce additional frictional losses

which may induce cycling behaviour. Furthermore, acoustic waves may be reflected, for example by an elbow, thus both changing the effective length of the first acoustic mode, and exacerbating potential water-hammer effects and the excitation of higher harmonics quicker. Nevertheless, it is at present not clear how to handle such issues at a fundamental, modelling or design level other than to replace the complex pipe geometry with an effective wavelength of the lowest-order acoustic mode and a damping or loss coefficient.

Based on experiments, Frommann and Friedel (1998) states that apart from a slight difference in the lift time history there is no noticeable difference if two bends were added to the inlet piping. In the case of complex pipe geometries, e.g. multiple side-branches, it is also possible to make predictions on the effect of geometrical parameters, see Tonon et al. (2011). For example Dequand et al. (2003) studies the acoustic response of a 90-degree sharp However, it is not clear at the moment how to merge such acoustic models with the valve and reservoir equations.

Although multi-device installation is often encountered in practice – to allow the stable venting of both small and large flow rates – it is rarely addressed in the literature. Among the few papers addressing this problem is Tamura et al. (2012b), where the PRVs are mounted onto stub pipes in a parallel way. The authors of this study address the flow-acoustic resonance at the T-junction of the main pipeline and the PRV stub line and find the unsteady vortices at the stub pipes generate acoustic resonance.

5.7. Vortex shedding

High-speed flow impinging on solid surfaces (e.g. the valve disc) or reaching open cavities like T-junctions Paál et al. (2006) or wedge-like obstacles Paál and Vaik (2007) might result in periodic vortex shedding, with well-defined frequencies that might excite the whole system. Note that such 'microscopic' flow properties are unlikely to result in instabilities *per se*. Since dynamic instability in terms of the quarter-wave coupling (or the Helmholz-like instability) do not rely on precise resonance, it would seem unlikely that particular vortex-shedding frequencies are likely to contribute to an instability mechanism.

Nevertheless, vortices may indeed be shed in the post-instability dynamics, and (in the case of gasses) there may be shock-waves too. That is, although these fluid-borne excitations may indeed be present in the dynamics, they are typically not the primary cause of valve chatter or flutter. It

is possible though that the transient shedding of vortices, for example during valve opening or closing, could provide an input of energy that would push an otherwise stable valve into a condition that would lead to instability. Indeed, Tamura et al. (2012b) studies the acoustic interaction between unsteady vortices and the pipeline system in detail.

5.8. Instability interactions

Although we have artificially separated the different instability mechanisms, in a real-life system they probably co-exist. For example, pressure and velocity oscillations during flutter might reach such large amplitudes that the valve pressure reaches blowdown pressure and rapid cycling will also occur. As shown by the measurement in Figure 7 in Hős et al. (2014), the chatter born during valve closing might not be simply killed by reaching the blowdown pressure but may survive to much lower vessel pressures. In the aforementioned measurement, the set pressure was 150 psi, the blowdown was just 5%, and yet the oscillation remained present until the vessel pressure fell beneath 90 psi. Another possibility we have seen is that valve jumps can cause transitions into or out of parameter regimes that are unstable to the quarter-wave instability.

In Bazsó et al. (2014), a two-parameter stability plot was produced for a simplified theoretical model. Here it is obvious that there are numerous parameter regions whose dynamics could only be understood by considering the interplay between grazing bifurcation, quarter-wave and Helmholtz instabilities.

6. Summary and Recommendations

6.1. Summary

The primary purpose of this paper has been to summarise and organise current understanding of the state of the art on direct spring-loaded pressure relief valve instabilities. The key messages can be summarised as follows:

1. Fundamentally speaking, it is not accurate to refer to a particular valve as being stable or unstable. Rather, it is the *system* — comprising the valve, the reservoir and the upstream (and, possibly, downstream) piping that may or may not develop an instability. Moreover whether or not an instability occurs depends on properties of the fluid and the operating conditions.

2. When trying to tease out whether a particular pressure release system is liable to become unstable, it is important to distinguish between fundamental, intrinsic instabilities and the triggering mechanisms that may be the precursor to the instability onset. It is our contention that any guidelines or standards should focus on preventing the conditions for fundamental instabilities – listed in Table 1 – to occur rather than concerning themselves with triggering mechanisms.
3. To this end, we have identified in Table 1 five different types of fundamental instability and produced simple design formulae for preventing them from occurring. We have tried through references and, in some cases through fresh analysis, to be completely transparent on the origins of these formulae and how the assumptions that lie behind them can be checked by others.
4. Of all these mechanisms, we argue that the quarter-wave instability is by far the most common and the most dangerous. This can be argued as flows. Oversized or underdamped valve instabilities essentially only occur due to a failure of the design process to identify the correct valve for the job at hand. The 3% rule is aimed at preventing cycling, rather than the more dangerous and prevalent flutter or chatter. Static valve jumps are a natural part of a valve's design and do not represent a dynamic instability in themselves. Finally, Helmoltz-mode oscillations are not likely to occur other than in installations with very small reservoirs and very short inlet pipes.
5. As for triggering mechanisms, we have analysed the so-called pressure surge criterion (18) which supposedly can predict the onset of chatter. This design criterion appears to be based on a simplified calculation of the pressure required for a valve to reseat once upon opening, rather than a stability analysis *per se*. Although this condition seems at best problematic in terms of a predictive tool for instability, we do note that it does contain the correct trend that the probability of instability increases with pipe length.
6. The dimensionless formula (15) for determining valves that are stable against quarter-wave instabilities shows promise. However, we should like to point out that it is more important to understand the theory that leads to this formula and the associate assumptions that underlie it. The key seems to be to avoid the negative damping provided by the valve of the quarter-wave acoustic mode.
7. In general we should like to advocate the approach adopted in this pa-

per. Mathematical modelling combined with careful experimental validation is a powerful tool for understanding the underlying physics. One needs a 'minimalist' mathematical model including only those physical effects that cause the instability. In contrast CFD is a great tool for studying particular dynamic scenarios, but it is not useful for parametric studies or qualitative understanding.

6.2. Recommendations

Rather than a series of detailed recommendations, which would not be appropriate for this scientific study, we shall propose here a number of approaches and investigations that we believe warrant further consideration.

6.2.1. Guidelines, standards and operating practice

In general, the authors encourage further discussion at industrial standard committee meetings globally with the goal of developing more appropriate guidelines to prevent instabilities in piping systems connected to relief valves. Such guidelines need parallel, independent and shared testing, both experimentally and via computer simulations. In particular, the existence evidence would point to the importance of having a criterion for preventing quarter-wave instabilities. In that direction we should like to point to not only to the simple formula (15) but also to the theory that underlies it.

6.2.2. Experimental validation

Understanding the instability types and the physical mechanisms is only the first step towards handling them and developing sizing and prevention rules. Any criterion or formula must be carefully validated by experiments. When designing such experiments, special care must be given to the *repeatability* of the tests. Our experience show that if the valve goes unstable and oscillates heavily, it will be very soon be badly damaged, notably galling appears on the shaft. Such galling, if not recognized, spoils further experiments (with the same valve) as it adds additional friction to the system which typically leads to spurious additional stability. Indeed, in the experiments reported in our earlier work, the shaft and the bushing of the test valves were carefully designed for repeatability.

6.2.3. The role of CFD

The speed, accuracy and range of applicability of computational fluid dynamics is rapidly developing. Unsteady fully three-dimensional transient

analysis with millions of grid points, incorporating complex turbulence models, which would have been a dream merely 10 years ago, are now feasible even on a standard desktop PC. Nevertheless, we do not recommend the use of CFD to develop fundamental design principles, advocating instead the approach of reduced-order modelling to capture the underlying physical mechanism concerned. Rather, CFD that has been carefully implemented and benchmarked against detailed experiments and low-fidelity studies can be used as a replacement for an extensive experimental campaign. Deforming grid, fluid-structure interaction, large-eddy simulation and multicomponent/multiphase technologies are nowadays available in commercial and open-source CFD codes 'out of the box'. These features can be useful in gaining further insight into transient and small-scale effects, as one is able to look in detail at flow features that would not be experimental observable. In addition, CFD can be used to calculate important properties such as discharge coefficients, loss factors and effective areas (or jet angles) that become coefficients of the simpler models or formulae. Finally, CFD will always be required as a validation tool for stand-alone cases with specialised fluids or geometries.

6.2.4. Gases vs. liquids and multiphase flow

Quite rightly, design standards and codes of practice differentiate clearly between compressible fluids (gases) and incompressible fluids (liquids). Interestingly, we have found that at a fundamental level there are few differences in terms of the instability mechanisms for PRV valve systems. Essentially, a gas service valve can be analysed with the same toolbox as a liquid one if the material properties are correctly evaluated at set pressure and correct exit-flow condition are taken into account. However, it is fair to say that the emphasis might be on different issues, for example water hammer effects are far more severe in liquids than in gases. These differences can be significant for both transient events, post-instability analysis and where more refined flow resolution is required.

Consideration of multiphase or multicomponent flow (e.g. water+steam or crude oil+gas+water) goes beyond the scope of the present study. While many of the fundamental mechanisms are likely to be similar, the additional complexities associated with fluid mixing are such that any general theory is likely to be quantitatively inaccurate. Hence, at present at least, we recommend single-case scenario analysis for such installations.

6.2.5. Validity of the 3 percent rule

The three percent rule (8) is designed to avoid instability due to inlet pressure drop, but it is absolutely unsuitable to predict any other instability type (quarter-wave, Helmholtz, etc.). As an example, any (reasonable) pipe diameter change plays only a marginal role in the quarter-wave instability as it does not affect the the wavelength of the quarter wave. Yet, the allowable pipe length according to the 3 percent rule changes heavily with the pipe diameter (for constant flow rate) – see Figure 7. Nevertheless, the 3% rule limits the inlet piping length, so its application might result in pipe lengths that are short enough to avoid quarter-wave coupling, but such cases are merely coincidence. Indeed, Frommann and Friedel (1998) finds, albeit based on a limited number of experiments, that the 3% rule is sufficient to avoid severe valve oscillations in case of an inlet line diameter equal to the safety valve inlet, but also adds *for most of the cases it is not sufficient.*

6.2.6. Validity of the pressure surge criterion

The pressure surge criterion (18) is based on a hybrid analysis that mixes steady force balance with highly dynamic effects (water hammer). Moreover, it concentrates on the first few milliseconds of valve opening. However, very often chatter occurs during closing or mid-lift, which clearly could not be explained using this approach. Moreover, the authors of the current paper feel that this sizing rule has not yet been rigorously validated either experimentally or in CFD. Note that, like the 3% rule, the pressure surge criterion suggests stability is improved for shorter inlet pipes. Therefore, it can be the case that a superficial application of this criterion could coincidentally suggest that it predicts stability. Therefore, we emphasize that a satisfactory validation should not simply report on whether the valve is stable or unstable during a test, but also gave actual pressure time histories at several locations along the pipe in order to check whether the reflected pressure waves are significant, and/or causal of the instability. One of the few such experiments was reported in Frommann and Friedel (1998), where the author finds that the pressure surge criterion *'may be insufficient'* to describe the process during opening, especially when using an intermediate inlet pipe with a wider diameter than that of the valve.

6.2.7. Complex pipeline geometries

Our present study considers only simple, straight, constant-diameter inlet piping without any side branches or junctions. It is important to take

further steps towards handling complex, real-life pipe layouts. One possible solution – besides expanding the LDM or the GDM, which is straightforward but results in slower computation – is to adjust the hydraulic impedance technique (see Wiley and Streeter (1978)). Such approach should also take into account the periodic excitations present in the system, e.g. due to reciprocating pumps. It is tempting to speculate, that in order to prevent quarter-wave-like instabilities one simply needs to calculate the effective length of the fundamental acoustic mode of the actually geometry. Nevertheless, there is a need for further investigation.

References

Aldeeb, A.A., Darby, R., Arndt, S., 2014. The dynamic response of pressure relief valves in vapor or gas service. Part II: Experimental investigation. Journal of loss prevention in the process industries 31, 127–132. doi:10.1016/j.jlp.2014.06.002.

Allison, T., Brun, K., 2015. Testing and modeling of an acoustic instability in pilot-operated pressure relief valves. Journal of Engineering for Gas Turbines and Power 138.

API-520, 2014. Sizing, selection and installation of pressure-relieving devices, American Petroleum Institute Standard 520, Revision II. Technical Report. API.

ASME-PTC25, 2014. Pressure Relief Devices, Performance Test Codes 25. Technical Report. Americal Society of Mechanical Engineers.

Bazsó, C., Champneys, A., Hős, C., 2014. Bifurcation Analysis of a Simplified Model of a Pressure Relief Valve Attached to a Pipe. SIAM Journal on Applied Dynamical Systems 13, 704–721.

Bazsó, C., Champneys, A., Hős, C., 2014. Bifurcation analysis of a simplified model or a pressure relief valve attached to a pipe. SIAM Journal on Applied Dynamical Systems 13, 704–721.

Bazsó, C., Champneys, A., Hős, C., 2015. Model reduction of a direct spring-loaded pressure relief valve with upstream pipe. IMA J. Appl. Math. 80, 1009–1024. Appeared ahead of print as doi: 10.1093/imamat/hxu034.

Bazsó, C., Hős, C., 2012. A CFD study on the stability of a hydraulic pressure relief valve, in: Proceedings of CMFF'12, pp. 428–434.

Bazsó, C., Hős, C., 2013. An experimental study on the stability of a direct spring loaded poppet relief valve. Journal of Fluids and Structures 42, 456–465.

Bazsó, C., Hős, C., 2015. On the static instability of liquid poppet valves. Periodica Polytechnica Mechanical Engineering 59, 1–7.

Beune, A., Kuerten, J., van Heumen, M., 2012. CFD analysis with fluid-structure interaction of opening high-pressure safety valves. Computers and Fluids 64, 108–116.

Bolin, C., Engeda, A., 2015. Analysis of flow-induced instability in a re-designed steam control valve. Applied Thermal Engineering 83, 40–47.

Burgess, J., 2015. Personal communication.

Chabane, S., Plumejault, S., Pierrat, D., Couzinet, A., Bayart, M., 2009. Vibration and chattering of conventional safety relief valve under built up back pressure, in: Proceedings of the 3rd IAHR International Meeting of the WorkGroup on Cavitation and Dynamic Problems in Hydraulic Machinery and Systems, pp. 281–294.

Chanaud, R., 1994. Efsfects of geometry on the resonance frequency of helmholtz resonators. Journal of Sound and Vibration 178, 337 – 348.

Cremers, J., Friedel, L., Pallaks, B., 2001. Validated sizing rule against chatter of relief valves during gas service. Journal of Loss Prevention in the Process Industries 14, 261–267.

CSB, 2016. US Chemical Safety Board. `http://www.csb.gov/`. Accessed: 2016-02-05.

Darby, R., 2012. The dynamic response of pressure relief valves in vapour or gas service. part 1: mathematical model. Proprietrary report for PERF 99-05.

Darby, R., Aldeeb, A.A., 2014. The dynamic response of pressure relief valves in vapor or gas service. Part III: Model validation. Journal of loss prevention in the process industries 31, 133–141. doi:10.1016/j.jlp.2014.06.001.

Dazhuan, W., Shiyang, L., Peng, W., 2015. {CFD} simulation of flow-pressure characteristics of a pressure control valve for automotive fuel supply system. Energy Conversion and Management 101, 658–665.

Dempster, W., Elmayyah, W., 2013. Two phase discharge flow prediction in safety valves. International Journal of Pressure Vessels and Piping 110, 61–65.

Dequand, S., Hulshoff, S., Aur, Y., 2003. Acoustics of 90 degree sharp bends . Part I : Low-frequency acoustical response. ?? 89, 1025–1037.

Erdődi, I., Hős, C., 2015. CFD simulation on the dynamics of a direct spring operated pressure relief valve, in: Proceedings of CMFF'15, Budapest. p. ??

Eyres, R., Champneys, A., Lieven, N., 2005a. Modelling and dynamic response of a damper with relief valve. Nonlinear Dynamics 40, 119–147.

Eyres, R., Piiroinen, P., Champneys, A., Lieven, N., 2005b. Grazing bifurcations and chaos in the dynamics of a hydraulic damper with relief valves. SIAM Journal on Applied Dynamical Systems 4, 1076–1106.

Frommann, O., Friedel, L., 1998. Analysis of safety relief valve chatter induced by pressure waves in gas flow. Journal of Loss Prevention in the Process Industries 11, 279–290.

Funk, J., 1964. Poppet valve stability. Journal of Basic Engineering 86, 207.

Galbally, D., García, G., Hernando, J., de Dios Sánchez, J., Barral, M., 2015. Analysis of pressure oscillations and safety relief valve vibrations in the main steam system of a boiling water reactor. Nuclear Engineering and Design 293, 258–271.

Green, W., Woods, G., 1973. Some causes of chatter in direct acting spring loaded poppet valve, in: The 3rd International Fliud Power Symposium, Turin, p. ??

Hős, C., Bazsó, C., Champneys, A., 2014a. Model reduction of a direct spring-loaded pressure relief valve with upstream pipe. IMA Journal of Applied Mathematics 80, 1009–1024.

Hős, C., Champneys, A., 2012. Grazing bifurcations and chatter in a pressure relief valve model. Physica D: Nonlinear Phenomena 241, 2068–2076. doi:10.1016/j.physd.2011.05.013.

Hős, C., Champneys, A., Paul, K., McNeely, M., 2014b. Dynamic behavior of direct spring loaded pressure relief valves in gas service: Model development, measurements and instability mechanisms. Journal of Loss Prevention in the Process Industries 31, 70–81.

Hős, C., Champneys, A., Paul, K., McNeely, M., 2014c. Dynamic behaviour of direct spring loaded pressure relief valves in gas service: model development, measurements and instability mechanisms. J. Loss Prevention Process Industries 31, 70–81.

Hős, C., Champneys, A., Paul, K., McNeely, M., 2015. Dynamic behaviour of direct spring loaded pressure relief valves in gas service: II reduced order modelling. Journal of Loss Prevention in the Process Industries 36, 1–12.

Hős, C., Champneys, A., Paul, K., McNeely, M., 2014. Dynamic behavior of direct spring loaded pressure relief valves in gas service: Model development, measurements and instability mechanisms. Journal of Loss Prevention in the Process Industries 31, 70–81.

Hős, C., Champneys, A., Paul, K., McNeely, M., 2016. Dynamic behaviour of direct spring loaded pressure relief valves: Iii valves in liquid service. To appear in *Journal of Loss Prevention in the Process Industries*.

ISO-4216, 2014. Safety devices for protection against excessive pressure — Part 1: Safety valves. Technical Report. International Organization for Standardization.

Izuchi, H., 2010. Stability analysis of safety valve. American Institute of Chemical Engineers, *10th Topical Conference on Natural Gas Uitilization ISBN: 9781617384417*.

Kasai, K., 1968. On the stability of a poppet valve with an elastic support : 1st report, considering the effect of the inlet piping system. Bulletin of JSME 11, 1068–1083.

Lax, P., Wendroff, B., 1960. Systems of conservation laws. Commun. Pure Appl Math. 13, 217237.

Leung, J., 2004. A theory on the discharge coefficient for safety relief valve. J. Loss Prevention Process Industries 17, 301–313.

Licskó, G., Champneys, A., Hős, C., 2009. Nonlinear Analysis of a Single Stage Pressure Relief Valve. International Journal of Applied Mathematics 39.

McCloy, D., McGuigan, R., 1964. Some static and dynamic characteristics of poppet valves, in: Proceedings of the Institution of Mechanical Engineers, Prof Eng Publishing. pp. 199–213.

Mehrzad, S., Javanshir, I., Ranji, A., Taheri, S., 2015. Modeling of fluid-induced vibrations and identification of hydrodynamic forces on flow control valves. Journal of Central South University 22, 2596–2603.

Melham, A., 2012. Prv stability requirements. Business confidential document by ioMosaic for 50th DIERS User Group Meeting, Concord Mass.

Melham, G., 2014a. Analysis of prv stability in relief systems, part i. detailed dynamics. An ioMosaic Corporation White Paper.

Melham, G., 2014b. Analysis of prv stability in relief systems, part ii. screening. An ioMosaic Corporation White Paper.

Misra, A., Behdinan, K., Cleghorn, W., 2002. Self-excited vibration of a control valve due to fluid-structure interaction. Journal of Fluids and Structures 16, 649 – 665.

Moussou, P., Gibert, R., Brasseur, G., Teygeman, C., Ferrari, J., Rit, J., 2010. Instability of pressure relief valves in water pipes. Journal of Pressure Vessel Technology 132.

Paál, G., Pinho, F., Maia, R., 2006. The effect of corner radius on the energy loss in 90 T-junction turbulent flows. The 13th International Conference on Fluid Flow Technologies , 470–477.

Paál, G., Vaik, I., 2007. Unsteady phenomena in the edge tone. International journal of heat and fluid flow 28, 575–586.

Press, W., Teukolsky, S., Vetterling, W., Flannery, B., 2007. Numerical Recipes The Art of Scientific Computing. Third ed., Cambridge University Press, New York, NY, USA.

Qian, J.Y., Wei, L., Jin, Z., Wang, J.K., Zhang, H., Lu, A.L., 2014. CFD analysis on the dynamic flow characteristics of the pilot-control globe valve. Energy Conversion and Management 87, 220–226.

Singh, A., 1982. An analytical study of the dynamics and stability of a spring loaded safety valve. Nuclear Engineering and Design 72, 197–204.

Singh, A., 1983. On the stability of a coupled safety valve-piping system. ASME American Nuclear Society ??, 29–37.

Smith, D., Burgess, J., 2013. An engineering method to mitigate the impact of regulatory focus on relief system installations by prioritizing risk, in: Proceedings of the 9th A. Chem. E. Global Congress on Global Safety, p. ?? Available to download from `SmithBurgess.com`.

Smith, D., Burgess, J., Powers, C., 2011. Relief device inlet piping: Beyond the 3 percent rule. Hydrocarbon Processing November, 59–66.

Song, X., Cui, L., Cao, M., Cao, W., Park, Y., Dempster, W., 2014. A CFD analysis of the dynamics of a direct-operated safety relief valve mounted on a pressure vessel. Energy Conversion and Management 81, 407–419.

Song, X.G., Park, Y.C., Park, J.H., 2013. Blowdown prediction of a conventional pressure relief valve with a simplified dynamic model. Mathematical and Computer Modelling 57, 279–288.

Srikanth, C., Bhasker, C., 2009. Flow analysis in valve with moving grids through CFD techniques. Advances in Engineering Software 40, 193–201.

Sverbilov, V., Stadnik, D., Makaryants, G., 2013. Study on dynamic behavior of a gas pressure relief valve fora big flow rate, in: Proceedings of the ASME. Bath Symposium on Fluid Power and Motion Control, 2013, ASME, Fluid Power Syst & Technol Div. p. ??

Tamura, A., Okuyama, K., Takahashi, S., Ohtsuka, M., 2012a. Development of numerical analysis method of flow-acoustic resonance in stub pipes of safety relief valves. Journal of Nuclear Science and Technology 49, 793–803.

Tamura, A., Okuyama, K., Takahashi, S., Ohtsuka, M., 2012b. Development of numerical analysis method of flow-acoustic resonance in stub pipes of safety relief valves. Journal of Nuclear Science and Technology 49, 793–803. doi:10.1080/00223131.2012.703943.

Tonon, D., Willems, J., Hirschberg, A., 2011. Self-sustained oscillations in pipe systems with multiple deep side branches: Prediction and reduction by detuning. Journal of Sound and Vibration 330, 5894–5912.

Urata, E., 1969. Thrust of poppet valve. Bulletin of The Japan Society of Mechanical Engineers 12, 10991109.

Wiley, E., Streeter, V., 1978. Fluid transients. volume 1. New York, McGraw-Hill International Book Co., 1978. 401 p.

Wu, D., Li, S., Wu, P., 2015. CFD simulation of flow-pressure characteristics of a pressure control valve for automotive fuel supply system. Energy Conversion and Management 101, 658–665.

Wylie, E., Streeter, V., 1993. Fluid transients in systems. Printice Hall, New Jersey.

Yao, Y., Zhou, H., Chen, Y., Yang, H., 2014. Stability analysis of a pilot operated counterbalance valve for a big flow rate, in: Proceedings of the ASME. Bath Symposium on Fluid Power and Motion Control, 2014, ASME, Fluid Power Syst & Technol Div. p. ??

Yonezawa, K., Ogawa, R., Ogi, K., Takino, T., Tsujimoto, Y., Endo, T., Tezuka, K., Morita, R., Inada, F., 2012. Flow-induced vibration of a steam control valve. Journal of Fluids and Structures 35, 76–88.

Zhang, D., Engeda, A., 2003. Venturi valves for steam turbines and improved design considerations. Proc. IMechE A: J. Power Energy 217, 219–230.

Zucker, D., Biblarz, O., 2002. Fundamentals of Gas Dynamics. John Wiley and Sons, New York.

Zucrow, M.J., Hoffman, J.D., 1976. Gas dynamics. volume 1. New York: John Wiley and Sons, 1976.

Appendix A. Dimensionless parameters and equations

We define reference frequency, dimensionless time, dimensionless displacement and pressure as

$$\omega_v = \sqrt{\frac{s}{m}}, \quad \tau = \omega_v t, \quad x_{\text{ref}} = \frac{A_{\text{eff}}(0)p_b}{s} = \frac{A_p p_b}{s} \quad \text{and} \quad \tilde{p} = \frac{p}{p_b}, \qquad \text{(A.1)}$$

that is, the time will be rescaled with the help of the valve eigenfrequency (i.e., the period of the valve free oscillation is 2π) and use the backpressure to rescale the pressure, i.e. the dimensionless backpressure is 1.

Appendix B. Dimensionless parameters

Using the above non-dimensionalisation, dimensionless spring precompression and damping can be defined by

$$\delta = \frac{x_0}{x_{\text{ref}}} \quad \text{and} \quad \hat{\kappa} = \frac{k}{\sqrt{sm}} \tag{B.1}$$

Using these new parameters turns the equation of motion of the valve into (B.8) and that of the reservoir pressure dynamics into (B.11). The mass flow rates and rescaled by the *capacity* of the valve $\dot{m}_{\text{cap}}$, which means that the flow rate parameter $q = \dot{m}/\dot{m}_{\text{cap}}$ ranges between 0 and 1 (or 0 – 100%). The reservoir size parameter appearing in (B.11) is

$$\beta = \frac{a^2\,\dot{m}_{\text{cap}}}{V_r \omega_v p_b} \tag{B.2}$$

and is inversely proportional to the reservoir size, i.e. small β value implies large reservoir. Two additional parameters also appear, namely

$$\mu = \frac{A_p \rho \omega_v x_{\text{ref}}}{\dot{m}_{\text{cap}}} \quad \text{and} \quad \sigma = \frac{C_d A_{ft}(x_{\text{ref}}) c_1 \sqrt{p_b}}{A_p \rho \omega_v x_{\text{ref}}} := \frac{\dot{m}_{\text{ref}}}{A_p \rho \omega_v x_{\text{ref}}}. \tag{B.3}$$

Performing similar transformation on the pipeline equations (see Appendix B.4 for details) gives the following parameters:

$$\varphi = \lambda \frac{x_{\text{ref}}}{D_p}, \quad \alpha = \frac{\rho A_p a}{m\omega} \quad \text{and} \quad \gamma = \frac{L\omega}{a}. \tag{B.4}$$

Here φ is the friction parameter, γ is the dimensionless pipe length and $\alpha\gamma$ is the ration of the mass of liquid (or gas) in the pipe and the valve mass. The eigenfrequency of the pipe is

$$f_{pipe} = \frac{a}{2L} = \frac{\omega}{2\gamma} = \frac{\pi f}{\gamma} \quad \rightarrow \quad \frac{f_{pipe}}{f_{valve}} = \frac{\pi}{\gamma}, \tag{B.5}$$

where f_{pipe} is the pipe eigenfrequency, f_{valve} is the valve eigenfrequency, i.e. for $\gamma = \pi$ the pipe and valve eigenfrequency match. Moreover, as explained in

details in Appendix C.2, we have resonance between the Helmholtz resonator formed by the pipe and reservoir and the valve provided that

$$1 = \frac{\beta\mu}{\alpha\gamma} = a^2\sqrt{\frac{A_p}{L_p V_r}}\frac{1}{\omega_v^2} = \frac{\omega_H^2}{\omega_v^2}. \tag{B.6}$$

Appendix B.1. Valve equation of motion

The equation of motion of the valve is

$$m\ddot{x}_v + k\dot{x}_v + s\left(x_v - x_0\right) = A_{eff}(x)\left(p_v - p_b\right) \tag{B.7}$$

We introduce $y_1 = x/x_{ref}$, $\tau = \omega_v t = \sqrt{s/m}t$ and $x_{ref} = A_{eff}(0)p_b/s = A_p p_b/s$. The pressures will be rescaled with the backpressure, i.e. $\tilde{p} = (p - p_b)/p_b$. The resulting new parameters will be (a) the dimensionless viscous damping is $\kappa = k/m/\omega$, (b) the dimensionless spring precompression $\delta = x_0/x_{ref}$ and the rescaled effective area curve $\tilde{A}_{eff} = A_{eff}(x)/A_{eff}(0)$. With these quantities, (B.7) becomes

$$y_1'' + \hat{\kappa}y_1' + (y_1 - \delta) = \tilde{A}_{eff}(y_1)\tilde{p}_v \tag{B.8}$$

for liquids. When dealing with gases we define $\tilde{p} = p/p_b$ resulting in

$$y_1'' + \hat{\kappa}y_1' + (y_1 - \delta) = \tilde{A}_{eff}(y_1)\left(\tilde{p}_v - 1\right). \tag{B.9}$$

Appendix B.2. Reservoir pressure dynamics

The general mass balance of the reservoir is

$$\dot{p}_r = \frac{a^2}{V_r}\left(\dot{m}_{r,in} - \dot{m}_{r,out}\right) \tag{B.10}$$

where p_r is the reservoir pressure, a is sonic velocity in the reservoir and V_r is the volume. $\dot{m}_{r,in}$ and $\dot{m}_{r,out}$ are the entering and leaving mass flow rates. Employing the previously defined dimensionless variables turns (B.10) into

$$\tilde{p}_r' = \beta\left(q_{in} - q_{out}\right), \tag{B.11}$$

where

$$\beta = \frac{\dot{m}_{ref}}{V_r\omega_v p_b\frac{1}{a^2}} \quad \text{and} \quad q_{in/out} = \frac{\dot{m}_{in/out}}{\dot{m}_{cap}}. \tag{B.12}$$

The mass flow rate scale $\dot{m}_{cap}$ can be arbitrarily chosen, we shall use the *valve capacity* as a reference value. In the case of liquids, the sonic velocity is $a^2 = E/\rho$ (E being the bulk modulus of the liquid) and hence β is straightforward to compute. However, in the case of gases, the sonic velocity is $a^2 = \gamma R T_r$ (with $\gamma = c_p/c_V$ being the ratio of heat capacities and R stands for the specific gas constant) and hence, if the reservoir temperature changes (e.g. due to the pressure change), β also changes. However, experiments show that constant reservoir temperature is an acceptable approximation.

Appendix B.3. Valve mass flow rate

In the case of valves in *liquid* service – see (1) – the flow through the valve is

$$\dot{m}_{v,liquid} = C_d A_{ft}(x_v) c_1 \sqrt{p_v - p_b}, \tag{B.13}$$

whose dimensionless form is

$$\begin{aligned}
\dot{q}_{v,liquid} = \frac{\dot{m}_{v,liquid}}{\dot{m}_{cap}} &= \frac{1}{\dot{m}_{cap}} C_d A_{ft}(x_v) c_1 \sqrt{(p_v - p_b)} = \\
&= \frac{1}{\dot{m}_{cap}} C_d \frac{A_{ft}(x_v) c_1}{A_{ft}(x_{ref})} A_{ft}(x_{ref}) \sqrt{p_b \left(\frac{p_v - p_b}{p_b} \right)} \\
&= \frac{C_d A_{ft}(x_{ref}) c_1 \sqrt{p_b}}{\dot{m}_{cap}} \tilde{A}_{out}(y_1) \sqrt{\tilde{p}_v} \\
&= \frac{A_p \rho \omega_v x_{ref}}{\dot{m}_{cap}} \frac{C_d \rho A_{ft}(x_{ref}) c_1 \sqrt{p_b}}{A_p \rho \omega_v x_{ref}} \tilde{A}_{out}(y_1) \sqrt{\tilde{p}_v} \\
&:= \mu \sigma \tilde{A}_{out}(y_1) \sqrt{\tilde{p}_v}
\end{aligned} \tag{B.14}$$

If the outlet area is $A_{ft} = D_p \pi x_v$, we have simply $\tilde{A}_{ft} = y_1$, which we shall use in what follows. The advantage of the above form is that the second term $\sigma y_1 \sqrt{\tilde{p}_v}$ represents the dimensionless fluid velocity in the pipe, at the valve-end. As explained in (3), for gas service we have formally the same equation but the constant is different, as for gases we have

$$c_1 = \sqrt{\rho_v \gamma \left(\frac{2}{\gamma + 1} \right)^{\frac{\gamma+1}{\gamma-1}}}, \tag{B.15}$$

where ρ_v is the average gas density at the valve.

Appendix B.4. Inertial pipe model

For incompressible liquids, the Bernoulli equation – augmented with the unsteady inertial term – reads

$$p_1 - p_2 = \lambda \frac{L}{D_p} \frac{\rho}{2} v \left| v \right| + \rho L \frac{\mathrm{d}v}{\mathrm{d}t} \tag{B.16}$$

which, after employing the above dimensionless parameters, turns into

$$\tilde{p}_1 - \tilde{p}_2 = \varphi \frac{\alpha\gamma}{\mu^2} q \left| q \right| + \frac{\alpha\gamma}{\mu} q' \tag{B.17}$$

in which

$$\varphi = \lambda \frac{x_{ref}}{D}, \quad \alpha = \frac{\rho A_p a}{m\omega}, \quad \gamma = \frac{L\omega}{a} \quad \text{and} \quad \mu = \frac{A_p \rho \omega x_{ref}}{\dot{m}_n}. \tag{B.18}$$

Here p_1 and p_2 are the (static) pressures at the beginning and end of the pipe, λ is the friction factor, L and D are the pipe length and diameter and $v(t)$ is the mean velocity in the pipe. Note that this model assumes plug-like flow, i.e. it takes into account the inertia of the liquid but does not model neither its compressibility, nor the wave effects.

Furthermore, φ is the friction parameter, α is the ratio of the inertial forces of the liquid and the valve, γ is the dimensionless pipe length and μ is the ratio of the reference mass flow rate ($v_{ref} = \omega x_{ref}$) and the nominal one. Moreover, it is worth mentioning that

$$\alpha\gamma = \frac{\rho A_p L}{m} = \frac{\text{mass of liquid in the pipe}}{\text{mass of the valve}}. \tag{B.19}$$

On the other hand, the eigenfrequency of the pipe is

$$f_{pipe} = \frac{a}{2L} = \frac{\omega}{2\gamma} = \frac{\pi f}{\gamma} \quad \rightarrow \quad \frac{f_{pipe}}{f_{valve}} = \frac{\pi}{\gamma}, \tag{B.20}$$

where f_{pipe} is the pipe eigenfrequency, f_{valve} is the valve eigenfrequency, i.e. for $\gamma = \pi$ the pipe and valve eigenfrequency match.

Appendix C. Stability of linear models

Appendix C.1. Close-coupled valve (CCV model)

In this model, we neglect the upstream piping, hence the valve pressure is approximately the tank pressure $\tilde{p}_e = \tilde{p}_v = \tilde{p}_r$. Let y_3 denote the relative

pressure above backpressure ($y_3 = \tilde{p}_v - 1$), then, in the case of liquid service, the governing equations (B.8) and (B.11) are reduced to

$$\begin{aligned} y_1' &= y_2 \\ y_2' &= -\kappa y_2 - (y_1 + \delta) + \tilde{A}_{eff}(y_1) y_3 \\ y_3' &= \beta \left(q - \mu\sigma y_1 \sqrt{y_3} \right) \end{aligned} \tag{C.1}$$

Provided that $A_{eff}(y_1) \equiv 1$ (i.e. the effective area curve is constant), the equilibrium of the above system satisfies $y_{1,e} + \delta = y_{3,e}$ and $q = \mu\sigma y_{1,e}\sqrt{y_{3,e}}$, which can be either solved numerically or, upon expanding the solution into Taylor series, we obtain the *explicit* approximating formula

$$y_{1,e} \approx \frac{\tilde{q}}{\sqrt{\delta}} - \frac{\tilde{q}^2}{2\delta^2} + \mathcal{O}(q^3) \quad \text{with} \quad \tilde{q} = \frac{q}{\mu\sigma}. \tag{C.2}$$

Standard linear stability analysis reveals that this equilibrium is on the threshold of stability if

$$\kappa_{crit} = \frac{\delta}{\beta q} \left(-\frac{\beta^2 q^2}{4\delta^2} - 1 \pm \sqrt{\left(\frac{\beta^2 q^2}{4\delta^2} + 1 \right)^2 + \frac{2\beta^2 \mu q \sigma}{\sqrt{\delta}}} \right) \tag{C.3}$$

The above formula can be expanded as a Taylor series for small flow rates, resulting in a simpler form, i.e.

$$\kappa_{crit}|_{\text{small q}} \approx \beta\sqrt{\delta}\mu\sigma - \frac{q}{2}\beta^3\mu^2\sigma^2. \tag{C.4}$$

The frequency of the appearing oscillation is

$$\omega^2 = 1 - \frac{\beta^2 \mu q \sigma \left(\beta^2 \mu q \sigma - 2\sqrt{\delta} \right)}{4\delta}, \tag{C.5}$$

which, for large reservoirs (small β values) is close to the valve eigenfrequency (which is 1 in terms of the dimensionless parameters).

Appendix C.2. Helmholtz model

In this case, we allow the presence of inlet piping, but we do not take into account the wave effects of its capacity, i.e. we employ the inertial pipe

model discussed in Appendix B.4. We have

$$\begin{aligned} y_1' &= y_2 \\ y_2' &= -\kappa y_2 - (y_1 + \delta) + \tilde{p}_v \\ y_3' &= \beta\,(q - y_4) \\ y_4' &= \frac{\mu}{\alpha\gamma}\,(y_3 - \tilde{p}_v) - \frac{\varphi}{\mu} y_4 |y_4| \quad \text{with} \quad \tilde{p}_v = \left(\frac{y_4}{\mu\sigma y_1}\right)^2 . \end{aligned} \tag{C.6}$$

Note that basically we have coupled a Helmholtz resonator (reservoir + pipe) to the valve model. Indeed, we have

$$y_3'' = -\beta y_4' = -\beta \frac{\mu}{\alpha\gamma} y_3 + \ldots , \tag{C.7}$$

which is a linear oscillator with eigenfrequency $\frac{\beta\mu}{\alpha\gamma} = a^2 \sqrt{\frac{A_p}{L_p V_r}} \frac{1}{\omega_v^2} = \frac{\omega_H^2}{\omega_v^2}$, where ω_H is the Helmholtz-frequency.